Using Microbubble Subharmonics to Non-Invasively Measure Internal Pressures

Hanna Michaelis

A thesis submitted in partial fulfillment of the

requirements for the degree of

Master of Science

University of Washington

2026

Committee:

Mike Averkiou

Tatiana Khokhlova

Thomas Matula

Program Authorized to Offer Degree:

Bioengineering

University of Washington

Abstract

Using Microbubble Subharmonics to Non-Invasively Measure Internal Pressures

Hanna Michaelis

Chair of the Supervisory Committee:

Mike Averkiou

Department of Bioengineering

Hydrostatic pressure measurements give healthcare providers essential information regarding patient health and are necessary for the diagnosis and treatment of many diseases. The current gold standard for these measurements is a catheterization procedure which is invasive and costly. A promising non-invasive alternative is to use ultrasound and microbubbles to monitor hydrostatic pressure by detecting changes in the subharmonic frequency component of the microbubble response to ultrasound. However, the relationship between subharmonic signal and hydrostatic pressure varies widely across microbubble formulations, experimental setups and acoustic parameters, limiting clinical implementation of the technique. SonoVue, a clinically approved contrast agent, is a promising option for this purpose, but there has been limited exploration of its hydrostatic pressure sensitivity compared to other agents, especially at low acoustic pressures. This thesis presents several investigations into the relationship between subharmonic signal and hydrostatic pressure utilizing both a single-element transducer bench-top setup and a modified clinical ultrasound system. **Chapter 1** introduces subharmonic imaging and its utilization for noninvasive hydrostatic pressure measurements. In **Chapter 2**, a single-element transducer bench-top setup was established to characterize the subharmonic response of SonoVue across a range of physiologically relevant hydrostatic pressures and acoustic parameters. In **Chapter 3**, optimal acoustic parameters were implemented on a clinical scanner and the mode's sensitivity to hydrostatic pressure across a range of acoustic pressures, microbubble concentrations, and agent formulations was evaluated. **Chapter 4** concludes with a summary of the accomplishments and future directions of the work. Together, these investigations represent a meaningful step toward a standardized, non-invasive framework for hydrostatic pressure estimation using clinically approved tools.

Table of Contents

Chapter 1. Introduction 1

1.1 Current Hydrostatic Pressure Measurements 1

1.2 Microbubble Physics and Nonlinear Acoustic Response 4

1.3 Subharmonic Signal Generation 6

1.4 Subharmonic-Aided Pressure Estimation 7

1.5 Effect of Microbubble Formulation and Concentration on Subharmonic Response 11

1.6 Motivations and Objectives 12

Chapter 2. Single-Element Transducer Experiments 14

2.1 Introduction 14

2.2 Methods 14

2.2.1 Experimental Parameter Selection and Rationale 14

2.2.2 Box Design and Fabrication 16

2.2.3 Experimental Setup and Alignment 18

2.2.4 Microbubble Preparation 20

2.2.5 Data Processing 21

2.3 Results 21

2.3.1 Validation of Subharmonic Signal and Pressure Sensitivity 22

2.3.2 Subharmonic Response Over Varying Acoustic Pressure 23

2.3.3 Subharmonic Response Over Varying Ambient Pressure 24

2.4 Discussion 25

2.4.1 Interpretation of Single-Element Findings 25

2.4.2 Key Experimental Insights 27

2.4.3 Limitations 27

2.4.4 Motivation for Clinical Machine Experiments 28

Chapter 3. Clinical Imaging System Experiments 29

3.1 Introduction 29

3.2 Methods 30

3.2.1 Clinical Imaging System Setup and Configuration 30

3.2.2 Pressurized Box Setup 31

3.2.3 Microbubble Preparation 31

3.2.4 Data Collection Procedure 32

3.2.5 Data Analysis 33

3.3 Results 33

3.3.1 Subharmonic Response of SonoVue Over Varying Acoustic Pressure 33

3.3.2 Subharmonic Response of SonoVue Over Varying Ambient Pressure 34

3.3.3 Effect of Concentration on Subharmonic Response 35

3.3.4 Comparison of SonoVue and Sonazoid 36

3.4 Discussion 37

3.4.1 Interpretation of Clinical Machine Findings 37

3.4.2 Comparison of SonoVue and Sonazoid 38

3.4.3 Concentration Effects 39

3.4.4 Comparison with Single-Element Findings 39

3.4.5 Limitations 40

Chapter 4. Discussion and Concluding Remarks 41

4.1 Summary of Main Findings 41

4.2 Subharmonic-Pressure Relationship 42

4.2.1 Comparison of SonoVue Results Across Setups 42

4.2.2 Microbubble Formulation Dependence 43

4.2.3 Comparison with Prior Literature 43

4.2.4 Implications for Parameter Standardization Across Scanners 44

4.3 Effect of Concentration on Subharmonic Response 45

4.4 Clinical Translation and Limitations 46

4.4.1 Successfully Conducting This Work on a Clinical Imaging System 46

4.4.2 Limitations 47

4.5 Future Work 48

4.6 Concluding Remarks 49

Table of Figures

Figure 1: Design of final box 18

Figure 2: Experimental setup of two single-element transducer experiment. 19

Figure 3: Bubbles in the box before and after experiment..... 21

Figure 4: Subharmonic response observed from reanalyzing the data in Keller et. al 22

Figure 5: Acoustic amplitude of subharmonic component and fundamental component of the frequency response at 150 kPa as ambient pressure increases. 23

Figure 6: Subharmonic response of SonoVue at 0 mmHg ambient pressure and varying acoustic pressure 24

Figure 7: Subharmonic magnitude vs ambient pressure at 75 kPa, 150 kPa and 300 kPa acoustic pressure. 25

Figure 8: Experimental setup for clinical imaging system 31

Figure 9: Subharmonic response of SonoVue in clinical system setup 34

Figure 10: Subharmonic response of SonoVue at a concentration of 10^4 mB/mL vs ambient pressure. 35

Figure 11: Response of SonoVue across concentrations 36

Figure 12: Sonazoid subharmonic response 37

Chapter 1. Introduction

Abstract

Hydrostatic pressure measurements are essential for diagnosing and managing a broad spectrum of medical diseases, including cardiac dysfunction, portal hypertension, cancer detection, cranial hypertension and more. The current gold standard for these measurements is a catheterization procedure, an invasive and potentially dangerous procedure that is especially inaccessible in low-resource settings. An alternative is to use microbubbles as a pressure sensor to monitor hydrostatic pressures throughout the body. The subharmonic response of microbubbles has been shown to be sensitive to ambient pressure, leading to the development of subharmonic imaging (SHI) and subharmonic-aided pressure estimation (SHAPE). Preliminary subharmonic pressure measurements, including clinical trials, have provided proof of concept for the idea; however, significant improvements need to be made, as the relationship between hydrostatic pressure and subharmonic magnitude is still widely debated, with many variables impacting the interaction. This chapter introduces the challenges with hydrostatic pressure measurements and why microbubble response may offer a better method.

1.1 Current Hydrostatic Pressure Measurements

The current gold standard to measure hydrostatic pressures is via a catheterization procedure that begins with creating an incision near a major vein, typically at the throat, arm or groin [1]. From there, a flexible tube with a balloon catheter near the tip is threaded from the incision, through major vessels, to the location of the pressure measurement [2]. These

measurements are completed in the heart [3], liver [4], tumors [5], the brain [6] and more. This is an invasive procedure that not all people have access to or are healthy enough to undergo. Risks include arterial thrombosis, infection, nerve damage, exsanguination, heart attack, and lung collapse [7]. A study performed by Connors et al. [8] found that heart catheterization in critically ill patients was associated with increased mortality and utilization of resources, although the cause of this was unclear. The inherent invasive nature of catheterization means it can only be performed in relatively high resource areas with access to a sterile surgical operating room, catheter guidewires, catheters, contrast dye and an imaging method to monitor throughout the procedure. Highly skilled individuals including cardiac surgeons, nurses, radiologists and more are also necessary for safe procedures.

The most common catheterization procedures are undertaken to measure arterial pressure in the heart, known as cardiac catheterization [9]. Pressures inside the heart are essential to monitor cardiovascular health, typically range from 0-100 mmHg and must be accurate within 5 mmHg [10]. The most common measurements are mean right arterial pressure which typically measure from 0-5 mmHg, right ventricular pressure from 1-30 mmHg and pulmonary arterial pressure between 4-30 mmHg [3]. The respective measurements in the left side of the heart are higher, but left side catheterization is less common as it is a much riskier procedure [11]. Cardiac pressure measurements are essential to diagnose coronary artery disease [11], heart failure [12], [13], pulmonary hypertension [14], and to evaluate ventricular function [15]. For those with pulmonary hypertension or other cardiovascular complications, knowing cardiac pressure can help determine if lifestyle changes or other interventions are effectively treating the disease. Complications due to cardiac catheterization include hematoma, pseudoaneurysm, thrombosis,

arrythmia, infection, stroke, myocardial infarction, and death [9]. The risk of major complications is typically less than 1% and death rates are about 0.05%, but with over 1 million procedures annually in the U.S. alone, this still means many people must deal with complications or are not strong enough to undergo the procedure [9].

Catheterization procedures are also commonly undergone to measure pressure in the liver, arteries and in the cranium. The most common procedure to measure pressure in the liver is hepatic venous pressure gradient (HVPG), which can be used to diagnose cirrhosis, portal hypertension and more [16]. For this procedure, a balloon catheter is inserted into the right jugular vein and then advanced to the right hepatic vein where two measurements are taken to calculate the HVPG [4]. Patients undergoing HVPG measurement typically present with pressures ranging from 0 to 40 mmHg, with normal values falling between 1 and 5 mmHg and values greater than 10 mmHg defining clinically significant portal hypertension [17]. Arterial pressures are used to identify patients with essential hypertension, although it is only commonly used when continuous pressure monitoring is required [18]. Intracranial pressure (ICP) monitoring is essential after traumatic brain injury and cranial hemorrhage [6]. The normal range for ICP is 7-15 mmHg and >20 mmHg is considered elevated, although in severe instances pressures can exceed 40-50 mmHg [6], [19].

Access to non-invasive pressure measurements would eliminate many of the risks that come with invasive surgery while also allowing for regular monitoring for people who have or are at elevated risk of the aforementioned diseases. A non-invasive alternative to catheterization would also increase access to pressure monitoring in low-resource settings where access to sterile surgical equipment, necessary specialists and required facilities are limited.

1.2 Microbubble Physics and Nonlinear Acoustic Response

Standard ultrasound involves the transmission of sound waves and detection of echoes generated by the reflection and scattering of sound within the body. This mode assumes linear propagation, meaning the echoed signal frequency is the same as the transmitted frequency [20]. However, ultrasound can also propagate non-linearly, resulting in additional frequencies at integer multiples of the fundamental frequency, known as harmonics [21].

Shelled microbubbles consist of a shell made of phospholipids, proteins or polymers, filled with an inert gas and ranging from 1 to 10 μm in diameter [22]. They are a vital tool in ultrasound imaging where they function as contrast agents. Microbubbles are approximately the size of a red blood cell but have a very different impedance than any particles that make up blood, allowing them to scatter sound very effectively [23]. This means that microbubbles enable blood flow visualization. Microbubbles are unique as an imaging contrast agent as they are a true blood pool agent, so they don't leak into tissue like contrast agents used in MRI or CT [23].

An ultrasound wave is sinusoidal in nature, alternating high and low pressures at a single frequency for a set pulse length. The signal sent by the ultrasound transducer is at a single frequency, known as the fundamental frequency. When insonified, microbubbles respond to low pressures by expanding and to high pressures by compressing. At very low acoustic pressures this expansion and compression are relatively symmetric and minimal so a microbubble oscillates at the same rate as the fundamental frequency [24].

Diagnostic ultrasound typically occurs at pressures between 0.6-3.5 MPa [25]. In this pressure range, the change in microbubble size is greater, causing nonlinearity. This occurs

because while a microbubble can expand to multiple times their original size, they can only compress a set amount [26]. This unequal expansion and compression result in additional frequency components in microbubble-reflected acoustic signals. These additional frequency components include harmonics, ultraharmonics and a subharmonic, and broadband noise, and are quantified relative to the fundamental frequency (f_0). Harmonics occur at every integer multiple of the fundamental frequency ($n \times f_0$, where n is an integer). Ultraharmonics and subharmonics occur at half integer multiples ($\frac{n}{2} \times f_0$, where n is an odd integer). The subharmonic specifically always occurs at half the fundamental frequency ($\frac{f_0}{2}$). Lastly, broadband noise is signal distributed to all frequencies. Sustained, periodic oscillations of microbubbles while maintaining their structural integrity and generating harmonics, ultraharmonics and a subharmonic is known as stable cavitation [27].

At high acoustic pressures beyond the diagnostic limits (>3.5 MPa), this oscillation becomes more unstable as microbubbles grow rapidly and then collapse violently, often destroying themselves. The violent collapse releases large amounts of energy in the form of shock waves, microjets and heat [27]. These effects have been harnessed therapeutically including improved drug delivery via sonoporation and bubble enhanced heating for tumor ablation [28]. In the frequency domain, inertial cavitation is often defined by the increase of broadband noise [29]. The exact threshold differentiating between stable and inertial cavitation is not well defined and varies based on the microbubble formulation and other acoustic factors [27].

The nonlinear response of microbubbles can be harnessed to isolate microbubble-specific signals in a technique called contrast enhanced ultrasound (CEUS). The magnitude of non-linear frequency components can be emphasized or minimized through unique pulsing schemes such as pulse inversion or amplitude modulation [20]. Different frequency components can also be altered by changing acoustic parameters, especially the driving frequency [29]. By setting the driving frequency to be twice the resonance of the microbubble, the acoustic threshold required to observe a subharmonic frequency decreases [30]. Subharmonic monitoring driven at twice the resonance frequency of the microbubble is especially useful in ambient pressure sensing as the subharmonic frequency specifically has a strong relationship with ambient pressure, which will be discussed in section 1.4.

1.3 Subharmonic Signal Generation

The subharmonic signal generated by phospholipid-shelled microbubbles is primarily dependent on both acoustic pressure and driving frequency [31]. In 1999, Shi et al [32] found that the subharmonic signal of Levovist bubbles when driven near their resonance frequency had a nonlinear relationship with acoustic pressure that underwent three stages: occurrence, growth, and saturation. The occurrence stage, which occurred at acoustic pressures <0.3 MPa, has a weak subharmonic response. The growth stage, which occurred from 0.3-0.6 MPa, showed a rapid increase in subharmonic amplitude, even over a relatively small change in acoustic pressure. Lastly, the saturation stage occurred at acoustic pressure >0.6 MPa. At this stage, the increase in subharmonic response leveled off, and broadband frequencies began to increase due to microbubble destruction. At the saturation stage there was also a low signal-to-noise ratio of

subharmonic signals. Later it was found that this relationship between subharmonic magnitude and acoustic pressure was highly dependent on microbubble formulation and transmit frequency [33].

Depending on the acoustic frequencies utilized to insonicate the microbubbles, the acoustic pressure required to generate a subharmonic signal changed [24], [34]. When driving the microbubbles at resonance frequency, higher acoustic pressures are necessary to obtain a well-resolved subharmonic signal. It is theorized that subharmonic generation from driving at resonance frequency occurs largely due to a combination of the collapse of resonant microbubbles as well as microbubbles oscillating at twice the resonance frequency [35]. Alternatively, when twice the resonance frequency is used, lower acoustic pressures can be used to generate a significant subharmonic signal [29]. At low acoustic pressures, microbubble shells experience a rapid change in effective surface tension as they transition from an elastic to a buckled state, resulting in compression preferential behavior [26]. Buckling behavior is influential in the production of a subharmonic. In this thesis, a transmit frequency of twice the resonance frequency of SonoVue was used, as low acoustic pressures reduce the risk of microbubble destruction and lipid shedding, which would lead to the occurrence of a free gas microbubble that preferentially expands in response to an ultrasound pulse.

1.4 Subharmonic-Aided Pressure Estimation

As the ambient pressure increases above atmospheric pressure, the oscillatory response of microbubbles changes. Specifically, three parameters will change: inhibition of expansion behavior, increased dissolution rate, and a shift in resonance frequency [36], [37]. During high

acoustic pressures (>0.6 MPa) and at twice resonance frequency, all three of these impacts are expected to be in play. Increasing the ambient pressure will dampen the impact of expansion behavior of large amplitude oscillation but also exaggerate the dissolution of microbubbles with ruptured shells, reducing the number of scatterers. Depending on how these effects are balanced, it is possible for the subharmonic signal to exhibit no change or even an inverse relationship with ambient pressure.

At lower acoustic pressures where no shell rupture is expected (<0.6 MPa), of the three parameters altered, only the resonance shift needs to be considered. The increase in ambient pressure at low acoustic pressures should emphasize compression-only behavior due to low initial surface tension, therefore increasing the subharmonic signal [38], [39].

These physical mechanisms of microbubble shell behavior underpin the varied relationships between subharmonic response and ambient pressure that have been observed across different agents and experimental conditions. Subharmonic dependency on ambient pressure was first studied in 1999 [30]. Shi et al [30] showed that when Levovist microbubbles were driven at resonance frequency at moderate to high acoustic pressure, the subharmonic response decreased linearly as ambient pressure increased. They found that all frequency components were impacted by the change in ambient pressure, but the subharmonic varied the most, motivating its continued study.

Future studies repeated this general idea with altered parameters. All studies done with Sonazoid also demonstrated a negative relationship between subharmonic amplitude and hydrostatic pressure, however, the sensitivity has varied significantly from 0.02-0.22 dB/mmHg

[38], [39]. Additionally, with all the experiments the experimental setups have varied widely, possibly contributing to the variety of results. Sonazoid also has been found to have distinct sensitivity depending on the hydrostatic pressure range, further contributing to the inconsistencies in literature and suggesting that the relationship between Sonazoid and hydrostatic pressure may actually be nonlinear. Definity has had very similar findings with a negative relationship between subharmonic and hydrostatic pressure but widely varying sensitivity [40], [41], [42].

The relationship between the subharmonic response of SonoVue and ambient pressure has been much more challenging to characterize, with even more widely varying results depending on the ambient pressure range and acoustic pressure used. At lower ambient pressure the relationship has been found to be linearly positive and then linearly negative, whereas with higher acoustic pressures only a negative linear relationship has been observed [36], [41], [43], [44], [45], [46]. It was also found that the response varied based on the time from preparation of the microbubble suspension, and that repeated pressure-depressurization cycles could also alter the response [47].

Many in vivo experiments have also been done to observe the feasibility of translating subharmonic pressure measurements into hemodynamic pressures. This includes measurements of the cardiopulmonary, portal, intracranial, bladder, tumor, interstitial, and compartment pressures. However, extensive work has only been done for cardiopulmonary and portal pressures. The first cardiopulmonary experiments were conducted by Forsberg et al., measuring aortic pressures in dogs with Sonazoid [48]. The measurements from this test were found to have reasonable degrees of accuracy, however, the procedure required a midline abdominal incision to

expose the aorta directly to the transducer due to the lack of an imaging system, limiting translatability and non-invasiveness. In 2012, subharmonic imaging modes began to be implemented as research options on ultrasound scanners, yet even now most of these modes remain research-only options. However, with this advancement, future research in canines did not require the invasive placement of the probe [49], [50]. For this research Sonazoid was once again used, and the signal successfully tracked pressure changes in both the left and right ventricle. However, a conversion factor had to be determined from an invasive catheterization procedure to measure absolute pressures [49], [50].

Clinical testing in subjects for cardiac catheterization first occurred in 2017 [51]. Cardiac ultrasound examination was conducted at the same time as cardiac catheterization, and the correlation between the subharmonic signal and catheter data was highly variable. Subsequent studies had an optimized acoustic pressure procedure and showed much improved correlation [52], [53], [54]. This was successfully done with both Sonazoid and Definity, although it is important to note that a conversion factor from a catheterization measurement was always required.

The first testing of portal pressures used an induced portal hypertension model in canines [55]. The subharmonic measurements were compared to catheter measurements, and the change in portal pressure after the induction of portal hypertension was found to have a moderate negative correlation with the change in subharmonic amplitude. Next, a clinical trial was done in patients planned for transjugular liver biopsy and HVPG measurements [56]. After the medical procedure, the portal and hepatic veins were scanned with subharmonic ultrasound and Sonazoid. It was found that patients with high HVPG had a higher subharmonic signal difference and that a

specific cutoff value allowed for prediction of HVPG > 10 with reasonable sensitivity and specificity. While these in vivo results demonstrate feasibility, the variability in sensitivity across agents highlights the need for a standardized experimental protocol.

1.5 Effect of Microbubble Formulation and Concentration on Subharmonic Response

As demonstrated in the literature reviewed above, the relationship between subharmonic intensity and ambient pressure varies widely depending on the microbubble formulation, acoustic pressure, acoustic frequency, and ambient pressure. Similarities have been found between some microbubble formulations, specifically Sonazoid and Definity, but SonoVue has remained an outlier. SonoVue exhibits a distinct biphasic behavior where the relationship between subharmonic amplitude and ambient pressure is positive at low acoustic pressures and negative at high acoustic pressures [26], [36], [38], [41], [43], [45], [46], [57].

Because different agents respond differently with different parameters, acoustic parameters that work well for one agent might not work well for another. Different groups evaluate different agents under different conditions and then often try to compare, leading to conflicting results. The lack of a standardized protocol makes it challenging to get a clear picture of the field or to find a ground truth that verifies a specific setup is effective.

Concentration has also varied much in previous studies, and prior work has shown that subharmonic amplitude is sensitive to agent concentration, with higher concentrations producing stronger subharmonic response. One study found an approximately 2.8-fold decrease in

subharmonic amplitude when concentration was reduced by an order of magnitude, a proportionally larger drop than was observed for the fundamental signal under the same conditions [58], suggesting that subharmonic imaging may be more sensitive to concentration changes than conventional contrast imaging [59]. The study referenced above was conducted with in-house microbubbles and concentration was not the intended variable of study, meaning more intentional research should still be done to identify if concentration has a nonlinear relationship in subharmonic mode, which would differ from other modes where the relationship has been shown to be linear [60].

1.6 Motivations and Objectives

Despite promising in vivo and clinical results, several barriers must be addressed before subharmonic pressure measurements can function as a fully standalone, non-invasive clinical tool. Barriers include the lack of consensus on optimal acoustic parameters and microbubble formulation across labs, the variability in subharmonic sensitivity across agents and experimental conditions, and the absence of a standardized, reproducible experimental protocol that can be translated directly to a clinical imaging system.

To address these concerns, this thesis proposes a robust experimental setup with tightly controlled acoustic parameters. It investigates SonoVue, an underutilized contrast agent in the field, and compares it to the more common Sonazoid. This is done via extensive parametric study utilizing both a highly controlled single-element benchtop experimental protocol and a modified clinical system that allows for real-time subharmonic imaging to test multiple acoustic pressures, ambient pressures and microbubble concentrations. All experiments were conducted in

vitro with acoustic parameters maintained below a mechanical index (MI) of 1.9, ensuring compliance with FDA guidelines for diagnostic ultrasound and direct translatability to a clinical imaging system [61]. Exceeding this limit increases the likelihood of acoustic pulses inducing bioeffects when translated to a clinical setting, and risks microbubble inertial cavitation, which can cause microbubble destruction and confound subharmonic measurements [62]. MI is defined by the equation $MI = p^{-}/\sqrt{f}$, where p^{-} is the peak negative pressure measured in MPa and f is the frequency measured in MHz.

This thesis is organized to reflect two phases of experimental work. In Chapter 2, SonoVue was driven at twice its resonance frequency with a single-element transducer, generating a subharmonic signal even at low acoustic pressures. Once established, the relationship between subharmonic amplitude and acoustic pressures from 75-800 kPa was systematically evaluated across ambient pressures spanning 0-150 mmHg. Chapter 3 translates these findings to a modified Philips EPIQ clinical ultrasound system. Subharmonic signal dependence on acoustic pressures from 70-700 kPa and ambient pressure from 0-80 mmHg was studied. Microbubble concentrations from $2.5x10^{2}$ to 10^{4} microbubbles/mL were analyzed along with both SonoVue and Sonazoid microbubbles. Chapter 4 synthesizes the findings from both phases, including a direct comparison of the two experimental setups. It also places the findings into a broader discussion of their implications for subharmonic pressure measurement optimization and clinical translation, followed by concluding remarks.

Chapter 2. Single-Element Transducer Experiments

2.1 Introduction

The experiments described in this chapter were designed to establish a reproducible bench-top framework for characterizing the relationship between subharmonic magnitude and ambient pressure under controlled in vitro conditions. A two-transducer single-element setup was used along with an airtight box, allowing precise control over all acoustic parameters without the use of an imaging system. The insights gained here directly informed the clinical machine experiments described in Chapter 3.

The goal of this phase of work was to validate that the experimental setup produces subharmonic signals consistent with prior literature and to establish a reproducible relationship between subharmonic magnitude and ambient pressure across a range of acoustic conditions. The tightly controlled setup allowed for independent variation of acoustic and ambient pressure parameters, enabling a more systematic characterization of the subharmonic response than is possible on a clinical imaging system.

2.2 Methods

2.2.1 Experimental Parameter Selection and Rationale

The experiments described in this chapter required careful selection of acoustic parameters to ensure that results would be both scientifically meaningful and translatable to a clinical imaging system. For cardiac imaging, a frequency between 4 and 7 MHz is commonly used [63]. A frequency of 4.4 MHz was selected for the following single element transducer

experiments as this is compatible with imaging methods and provides sufficient separation between the fundamental and subharmonic frequencies. This driving frequency is also approximately twice the resonance of SonoVue microbubbles [64]. This was chosen to minimize the acoustic pressure required for subharmonic generation. For these experiments, 40 cycles were used to ensure sufficient frequency resolution to clearly distinguish the subharmonic from neighboring frequency components.

A V307 single-element transducer (Olympus NDT, Waltham, MA, USA) was selected for transmission and a C304 transducer (Olympus NDT, Waltham, MA, USA) for reception. The V307 has a center frequency of 5 MHz but was run at 4.4 MHz for these experiments to more closely reflect what a clinical imaging system would use. The C304 has a center frequency of 2.25 MHz and a focal distance of 7.6 cm, which was well suited for receiving near the expected subharmonic frequency of 2.2 MHz.

Prior to experiments, the V307 was characterized to verify that its actual output matched the specifications required for this work, as manufacturer specifications can differ from measured values. The V307 was placed in a large water tank and connected to a 3D positioner. A membrane hydrophone (UT1604-225; Precision Acoustics, Dorchester, UK) was used to measure the pressure field of the transducer. The transducer and hydrophone were first aligned axially by monitoring time of flight and using the known speed of sound in water to calculate axial distance. A previously built LabVIEW virtual instrument (VI) was then used to take propagation curves and beam patterns by stepping the 3D positioner through a set range in the axial and transverse directions respectively. A pressure calibration curve was also taken. These measurements led to the determination that 8 cm from the V307 face was the ideal distance for

scattering experiments, and that the transducer emitted pressures at a rate of 3 kPa/mV. Tests were also conducted to confirm that transmitting at 4.4 MHz rather than the designed 5 MHz did not have a major impact on acoustic pressure output. Impedance matching was tested and found to not be effective for this setup.

2.2.2 Box Design and Fabrication

The pressurized box used in all experiments was designed to meet several critical requirements: it had to be fully airtight and capable of withstanding internal pressures up to 150 mmHg without leaking or structural deformation, fillable and drainable with a water-microbubble solution, and acoustically transparent to allow the ultrasound beam to pass through without significant reflection or impedance. To allow precise transducer alignment, the box also had to fit within the constraints of the water tank (41x37x28 cm) while maintaining the foci of both transducers within the box interior. Two iterations of the box were designed and machined from acrylic, with the second iteration used in all experiments described in this thesis.

The box had two channels that allowed for attachment of a syringe and a pressure gauge, sealed to withstand elevated ambient pressures for extended periods. The box was designed from scratch, beginning with hand drawings and then translated into a 3D CAD design in SolidWorks before being machined.

The corners of the box were made airtight using SCIGRIP 4 (IPS Corporation, Durham, NC, USA), an acrylic cement that welds the walls together so that they fuse, making the bond as strong as the acrylic itself. The windows were attached with silicone, creating an airtight seal. Filling and drainage of the box happened via the two channels attached to rubber tubing on the

top of the box. To fill the box, one tube was attached to a syringe with a Luer lock with the plunger completely down, separated by a three-way stopcock. The other tube was placed in a beaker with the water-microbubble solution. By pulling the plunger on the syringe while the stopcock was closed, a vacuum was created, pulling the solution into the box. Once flow was established, opening the stopcock allowed for continued flow from the beaker into the box.

Sound transparency was achieved by including windows made of mylar, a material that is relatively acoustically transparent. Calculations using the KZK equation confirmed that the sound beam was smaller than the window at the relevant transducer distances, ensuring the beam could pass through with minimal impedance.

The first iteration of the box was sized 9x9x10.5 cm with rectangular windows on three sides (5x6 cm), 0.75 cm thick acrylic, and mylar film windows (0.13 mm thickness) along with a holding post attached near the edge of the box. This design experienced window bulging when pressurized and could not consistently withstand high pressures. The second iteration addressed these issues with circular windows of 5 cm diameter, 1 cm thick acrylic, dimensions of 9x9x10 cm, and a holding post attached to the middle of the top to reduce torque. This second box also contained an internal miniature stir bar which allowed for continual stirring during data capture and was used in all experiments described in this thesis.

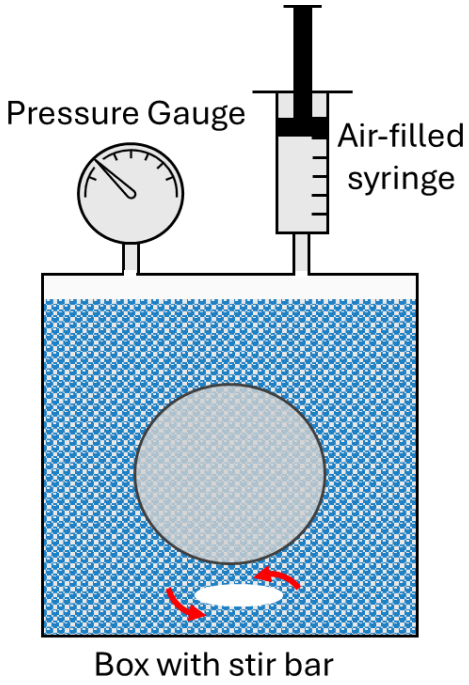

Figure 1: Design of final box

2.2.3 Experimental Setup and Alignment

The experimental setup consisted of the airtight box fully submerged in degassed, deionized water (Figure 2a). The two selected transducers (V307 and C304) were aligned at the center of the box at a 90-degree angle (Figure 2b). Alignment was achieved by first placing a copper wire at the intended center of the box and using motorized and non-motorized stages to position the transducers within 0.1 mm of the specified focal distance. Each transducer was aligned individually: first in the axial direction by monitoring time of flight, and then in the azimuthal direction by scanning left to right until the received signal was maximized. The two transducers were then aligned to each other on the elevation axis.

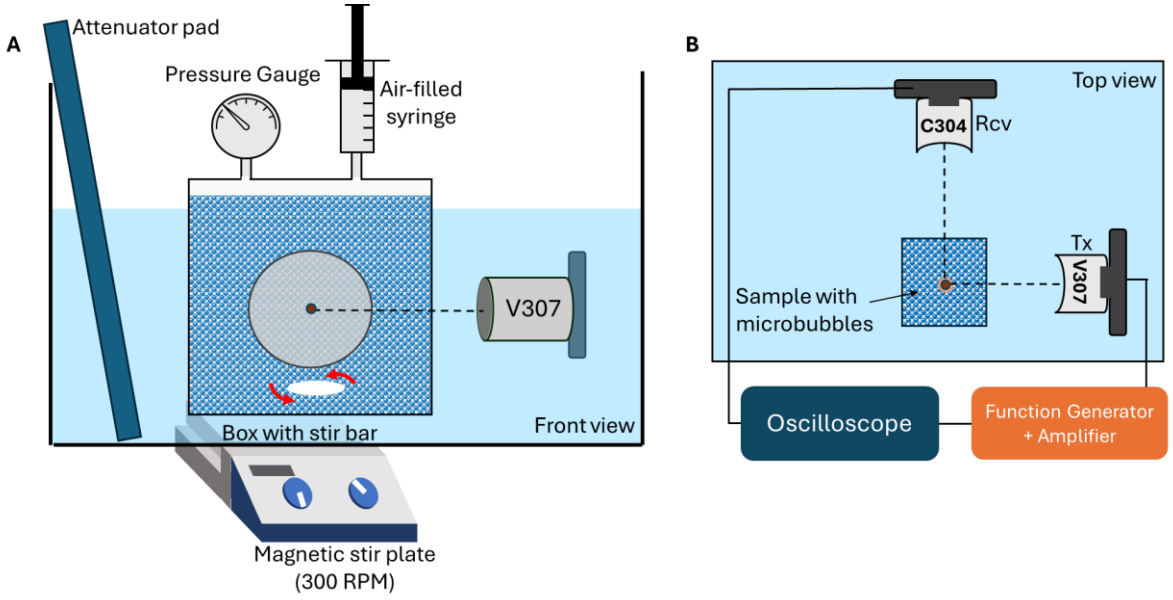

Figure 2: Experimental setup of two single-element transducer experiment. A) Front View B) Top View

Once aligned on the wire, the wire was replaced with the box, which was filled with a mixture of deionized water and microbubbles. After the box was submerged, a pulse of 40 cycles at 4.4 MHz was generated using an arbitrary function generator (AFG3102C, Tektronix, Beaverton, OR, USA) and a LabVIEW VI. PI was utilized, and each trial consisted of 50 PI pulse pairs, resulting in 100 total pulses. The response of the microbubbles was measured by the C304 transducer connected to an oscilloscope (DPO 7054C Tektronix, Beaverton, OR, USA). Each experiment was run at N=3, resulting in 150 total PI pulses across 3 trials.

To ensure that the PI VI worked as expected, results from performing PI manually and via the VI were compared. Both methods gave comparable results, reducing the size of the fundamental signal to the level of noise.

2.2.4 Microbubble Preparation

For each day of experiments a new vial of SonoVue microbubbles (Bracco Suisse SA, Geneva, Switzerland) was prepared by suspending the contents in saline according to the manufacturer's instructions. A concentration of 10^4 microbubbles/mL was prepared by withdrawing 0.1 mL from the reconstituted vial and adding it directly to 1 L of deionized water. Once prepared, the solution was stirred for 30 seconds before being siphoned from the beaker into the pressurized box. During siphoning, the beaker was gently and continuously agitated to ensure a uniform microbubble distribution. In early experiments, microbubbles were imaged before and after siphoning to confirm that the transfer process did not adversely affect microbubble integrity. Contrast-enhanced ultrasound imaging was also performed to verify microbubble concentration within the box prior to each experiment. Suspension time was carefully monitored and the time from vial to box was always kept to 3 minutes. Additional imaging was also completed before and after experimentation to ensure bubble concentration remained consistent (Figure 3).

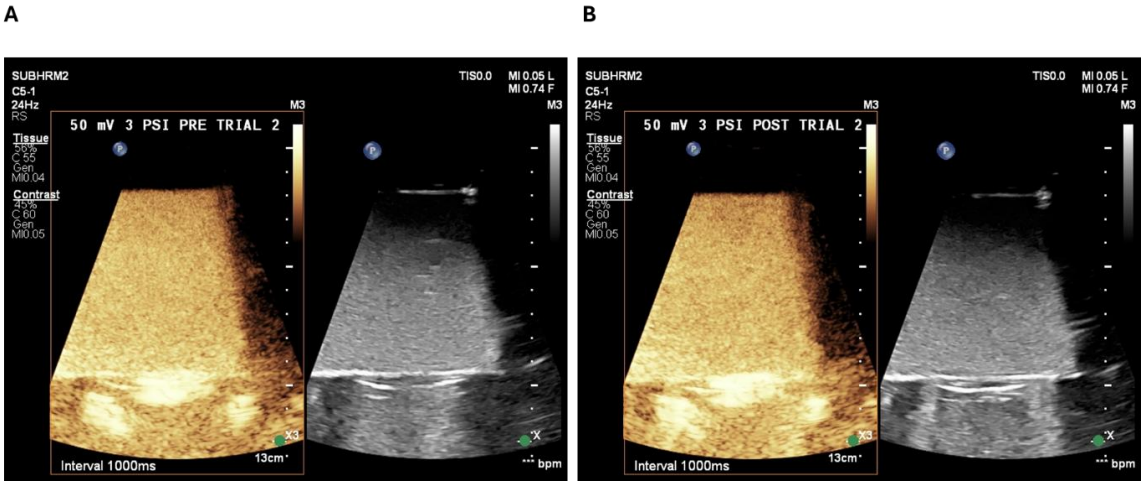

Figure 3: Bubbles in the box before and after experiment. Bubble concentration and quality remained the same. A) Before experiment. B) After experiment

2.2.5 Data Processing

All data collected from single-element transducer experiments was processed in MATLAB (Mathworks). Once loaded, the signal was truncated to the pulse length (90 µs) in the time domain. Each signal was then multiplied by a Blackman-Harris window in the time domain before calculating a one-sided frequency spectrum. This was created by taking an FFT of the truncated data, taking only the first half of this frequency spectrum, and then scaling by 2/N to normalize with respect to 1 mV. This process was repeated for all pulses (N=50 regular pulses, N=50 inverse pulses). PI was then applied by multiplying respective FFTs by ½ and adding them together. The magnitude of the subharmonic was recorded by extracting the FFT value at the expected subharmonic frequency of 2.2 MHz.

2.3 Results

2.3.1 Validation of Subharmonic Signal and Pressure Sensitivity

To validate that subharmonic magnitude changes with acoustic and ambient pressure, existing data gathered by the lab and published by Sara Keller [65] was first reprocessed to specifically observe this relationship. New code was developed in MATLAB to process this data with a focus on the subharmonic. Once processed, a positive relationship was observed between acoustic pressure and subharmonic magnitude, and a general S-curve shape comparable to results shown in the literature was seen [30] (Figure 4). Observing this relationship in data that was not originally designed for subharmonic evaluation was promising, as it indicated that an even stronger relationship would be obtained with a subharmonic-specific setup.

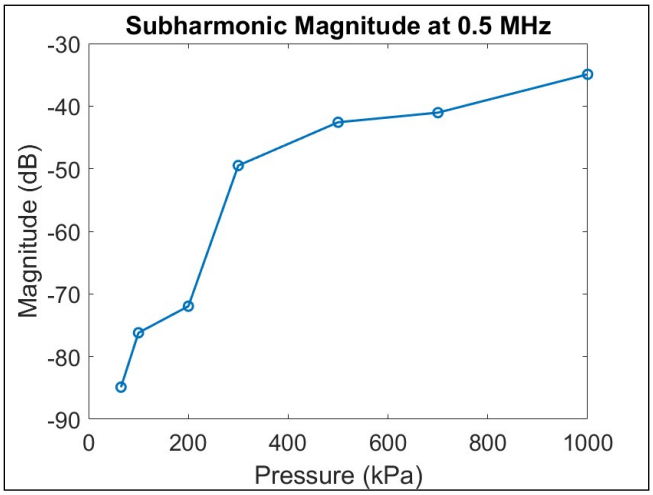

Figure 4: Subharmonic response observed from reanalyzing the data in Keller et. al. As acoustic pressure increases, subharmonic amplitude also increases nonlinearly

To validate that the subharmonic is more sensitive to ambient pressure than the fundamental, additional testing was done utilizing the setup described in Section 2.2.3. When insonicated at 150 kPa the subharmonic frequency component of the microbubbles increased to

7.5 dB at 50 mmHg, 8.7 dB at 100 mmHg and went back down to 5.1 dB at 150 mmHg compared to the response at atmospheric pressure. The respective measurements for the fundamental signal were only 1.9 dB, 0.4 dB and 2.9 dB (Figure 5). This indicated that the subharmonic amplitude was more sensitive to ambient pressure changes than the fundamental.

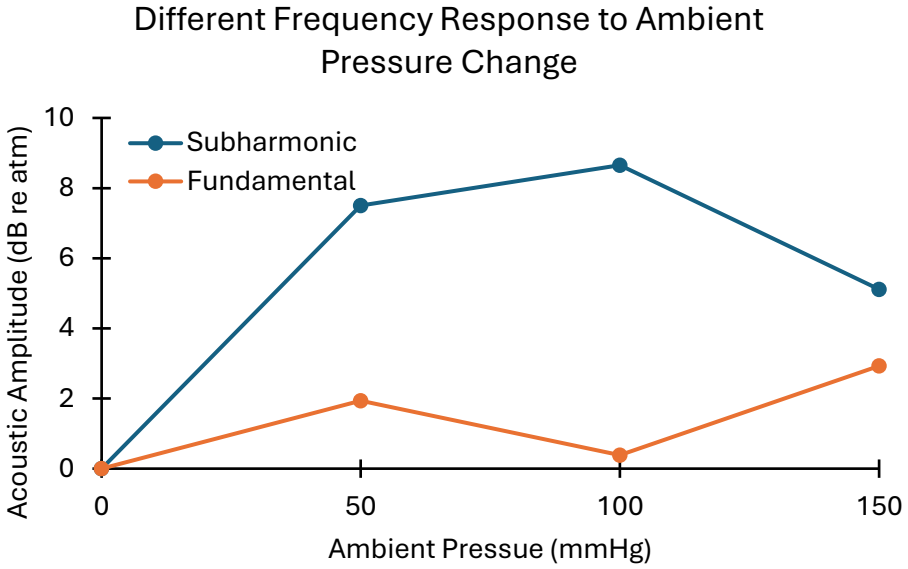

Figure 5: Acoustic amplitude of subharmonic component and fundamental component of the frequency response at 150 kPa as ambient pressure increases. Subharmonic component changes much more as the ambient pressure changes.

2.3.2 Subharmonic Response Over Varying Acoustic Pressure

To confirm that the new single-element setup produces the characteristic S-curve behavior described in literature, scattering experiments were conducted over a range of acoustic pressures. The three characteristic stages of the S-curve were all observed. The occurrence stage was seen from 100 to 300 kPa, growth from 300 to 500 kPa, and saturation from 500 to 800 kPa (Figure 6).

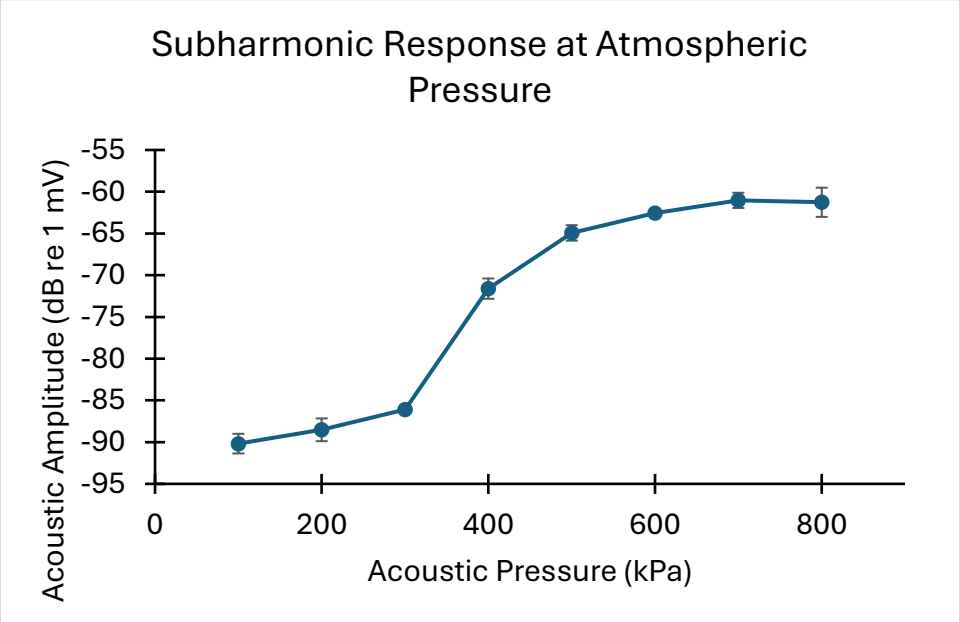

Figure 6: Subharmonic response of SonoVue at 0 mmHg ambient pressure and varying acoustic pressure. Three stages of subharmonic response are visible, occurrence from 50-300 kPa, growth from 300-550 kPa and saturation from 550-800 kPa.

2.3.3 Subharmonic Response Over Varying Ambient Pressure

The magnitude of the subharmonic signal was observed from 0 to 150 mmHg ambient pressure at a step size of 50 mmHg, at three acoustic pressures: 75, 150, and 300 kPa. A similar trend was observed across all three acoustic pressures: the subharmonic magnitude increased from 0 to 50 mmHg, plateaued from 50 to 100 mmHg, and decreased from 100 to 150 mmHg.

The subharmonic magnitude was maximized at an acoustic pressure of 150 kPa, where it reached a magnitude of 8.65 dB re atmospheric pressure (Figure 7). This indicated that very high acoustic pressures risk inertial cavitation and microbubble destruction, while low acoustic pressures do not excite the microbubbles sufficiently to generate a well-defined subharmonic signal.

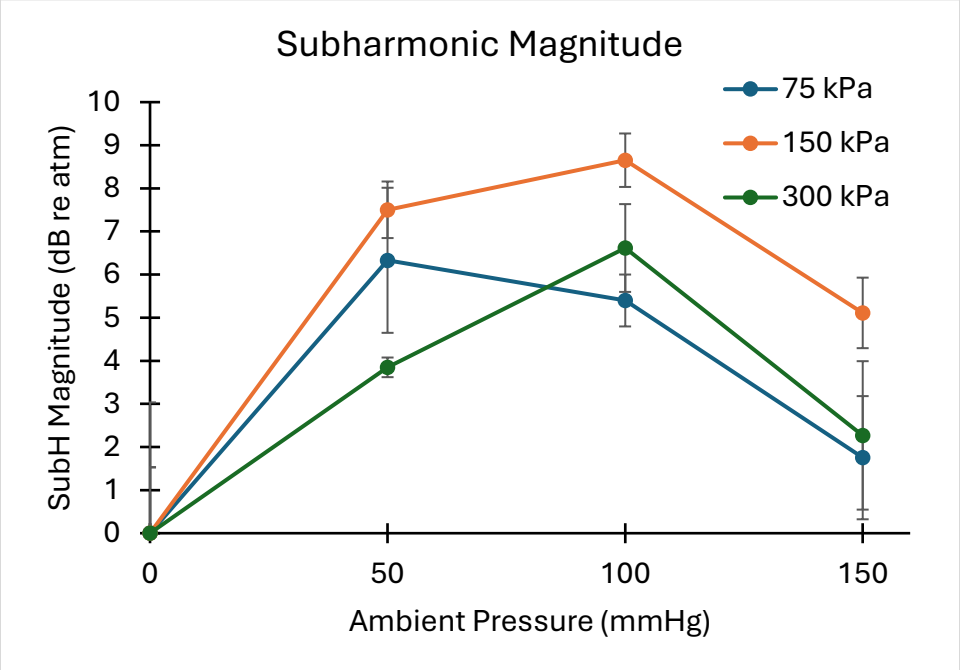

Figure 7: Subharmonic magnitude vs ambient pressure at 75 kPa, 150 kPa and 300 kPa acoustic pressure. Moderate acoustic pressure condition maximizes sensitivity

2.4 Discussion

This chapter demonstrated that the subharmonic response of SonoVue microbubbles is sensitive to ambient pressure changes under controlled in vitro conditions. Through careful control of experimental variables, a reproducible method for evaluating subharmonic signals was established using a single-element transducer setup.

2.4.1 Interpretation of Single-Element Findings

The most significant finding from this phase of the work is the predictable, non-linear relationship between ambient pressure and subharmonic magnitude for SonoVue. Prior studies had produced mixed results, finding relationships ranging from positive to null to negative

depending on the experimental conditions used. The experiments described here clarified this relationship for SonoVue by tightly controlling key variables and utilizing pulse inversion to suppress the fundamental signal.

This relationship between ambient pressure and subharmonic magnitude was observed to be positive from 0-100 mmHg and negative from 100-150 mmHg. This aligns with increasing ambient pressure causing more buckling behavior of the microbubbles up to a point [26], [38]. At very high ambient pressures this levels off and then decreases, likely due to the high pressure causing disruption to the microbubble shell. This was observed in conjunction with an S-curve with increasing acoustic pressure, aligning with literature. This provides reinforcement for previously hypothesized signal dynamics under stable cavitation.

The discovery that high acoustic pressures result in degradation of the subharmonic signal reinforces the importance of utilizing low acoustic pressures for effective subharmonic pressure sensing. At high acoustic pressures the subharmonic signal was swallowed by broadband noise, making it impossible to differentiate the two.

The experimental design also successfully met all physical design requirements. The airtight pressurized box withstood pressures up to 150 mmHg without leaking or structural compromise, achieved through an iterative design process and careful material selection. The inclusion of a stir bar in the second box iteration ensured microbubble uniformity throughout the experiment and improved signal reproducibility. The MI of the setup remained below 1.9 at all acoustic pressures used, reaching a maximum of approximately 1.4 and ensuring that results are directly translatable to a clinical setting.

2.4.2 Key Experimental Insights

Several experimental observations have direct implications for the design of the clinical machine experiments in Chapter 3. First, microbubble suspension time was found to have a significant impact on the subharmonic-ambient pressure relationship. When suspension time increased from three to eight minutes, the observed trend changed substantially, underscoring the need for strict timing protocols in all subsequent experiments.

Additionally, it was found that when driving at twice the resonance frequency of SonoVue, it is possible to generate a well-defined subharmonic at relatively low acoustic pressure, limiting microbubble destruction. Also, using pulse inversion can effectively minimize the fundamental frequency without eliminating the subharmonic. This validates the use of PI to better differentiate the subharmonic signal from the fundamental.

2.4.3 Limitations

The studies described in this chapter are limited by their in vitro nature. The use of a pressurized chamber placed in a water tank allowed for direct assessment of freshly prepared microbubbles across a wide range of acoustic conditions with tightly controlled concentrations. However, this eliminates several complications present in vivo. In the body, large microbubbles are filtered by the lungs and microbubble dissipation rate is altered, both of which could influence results. The setup also lacks the physiological flow present in the body, which continuously replenishes the microbubble population within the imaging plane and exposes microbubbles to dynamically changing pressures rather than the static pressures applied here. Additionally, only a single microbubble formulation and a limited range of concentrations were investigated at this stage.

This method also still lacks the ability to measure absolute pressures. While it establishes that the subharmonic response of SonoVue is sensitive to ambient pressures, this current system still only has the ability to measure relative pressure, not absolute. This means that there is still limited clinical viability, as absolute pressures are necessary for diagnosis of disease.

2.4.4 Motivation for Clinical Machine Experiments

The results from this chapter establish that a consistent and reproducible subharmonic pressure relationship can be achieved under tightly controlled bench-top conditions. However, for this technique to have clinical utility, it must be demonstrated on a clinical imaging system with real imaging hardware, a wider range of microbubble formulations and concentrations, and under conditions more closely resembling clinical use. Chapter 3 directly builds on the protocols established here — including suspension time, concentration ranges, and acoustic pressure selection — and translates them to a Philips EPIQ clinical imaging system with a C5-1 transducer, using both SonoVue and Sonazoid microbubbles.

Chapter 3. Clinical Imaging System Experiments

3.1 Introduction

The experiments described in this chapter build directly on the single-element transducer work presented in Chapter 2. While the bench-top setup allowed for precise control of acoustic parameters and validated a reproducible subharmonic-pressure relationship for SonoVue under tightly controlled conditions, it relied on specialized single-element equipment that is not representative of a clinical environment and doesn't allow for real-time imaging. The next step toward clinical translation is to demonstrate that these findings hold on a real clinical imaging system, using clinically relevant hardware and protocols.

This chapter describes experiments conducted on a modified Philips EPIQ ultrasound system, pursuing three goals. The first is to successfully translate the subharmonic-pressure relationship established in Chapter 2 to a clinical imaging platform. Second, investigate whether microbubble concentration is a meaningful confounding variable for the subharmonic-pressure relationship. Third, compare the subharmonic pressure sensitivity of SonoVue and Sonazoid under identical experimental conditions, directly addressing the lack of cross-agent comparison in the existing literature.

The chapter is organized as follows: Section 3.2 describes the methods used including the clinical system configuration, microbubble preparation, and data analysis procedures. Section 3.3 presents the results for SonoVue across acoustic pressure, ambient pressure, and concentration,

followed by a comparison with Sonazoid. Section 3.4 discusses the findings and their implications.

3.2 Methods

3.2.1 Clinical Imaging System Setup and Configuration

All clinical imaging experiments were conducted using a modified Philips EPIQ ultrasound system (Philips Healthcare, Bothell, WA, USA) paired with a C5-1 phased array transducer (Philips Healthcare, Bothell, WA, USA). The system was configured with a transmit center frequency of 4.2 MHz and a receive frequency of 2.1 MHz, corresponding to the subharmonic of the transmitted pulse. Acoustic pressures ranged from 70-700 kPa and ambient pressures from 0-80 mmHg. A pulse repetition frequency (PRF) of 1 Hz was used with 18 cycles per pulse. All imaging was performed in a modified research mode developed specifically for subharmonic acquisition at these frequencies.

The imaging depth was set to 12 cm which minimized acoustic reflections from within the box. The focal depth was fixed at 5 cm, corresponding to the center of the pressurized box. The dynamic range was set to 70 and the gain was changed throughout the procedure to avoid saturation. Any changes made to the gain were accounted for in processing to ensure all subharmonic intensities were normalized. An acoustic attenuator pad was placed behind the box within the water tank to absorb residual acoustic energy and reduce reflections within the water tank. A 7-liter water tank was used with the same pressurized acrylic box described in Chapter 2. The C5-1 transducer served as both transmitter and receiver for all measurements.

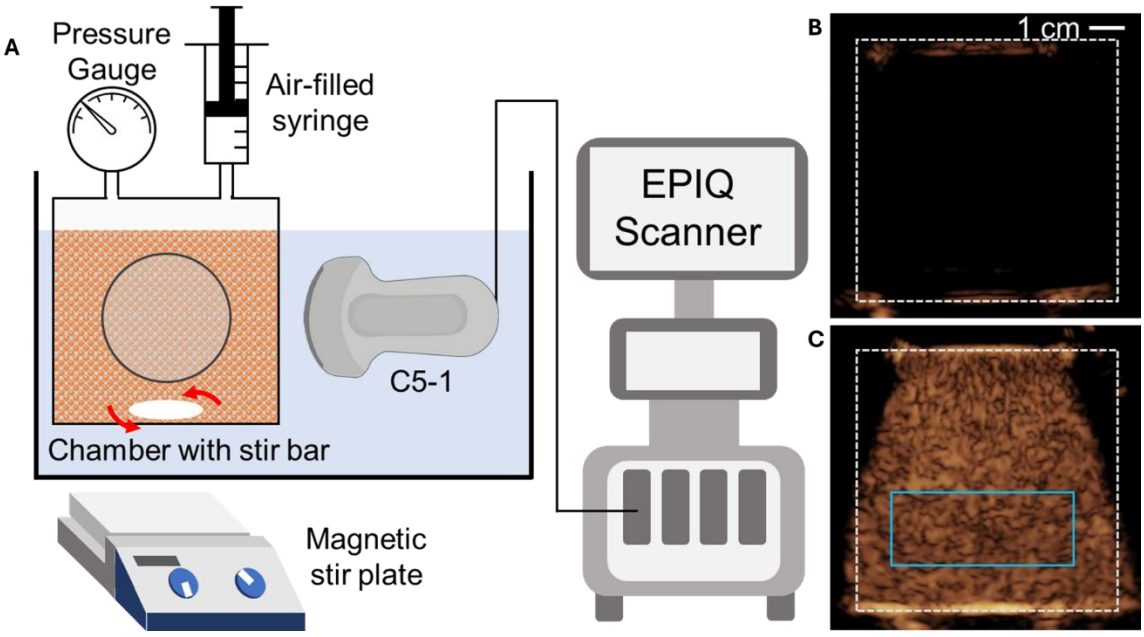

Figure 8: A)Experimental setup for clinical imaging system. B) Image taken when no microbubbles are in the box. Minimal reflections appear in the setup. C) ROI used to analyze images

3.2.2 Pressurized Box Setup

The same pressurized acrylic box described in Section 2.2.2 was used for all clinical machine experiments. The box was placed in the 7-liter water tank and aligned using imaging to ensure the center of the box was placed at the 5 cm focal depth. The box was angled slightly, by ~5 degrees, to help minimize reflections from the face of the box returning to the transducer. Ambient pressure was applied and monitored using a syringe and pressure gauge connected to the box via the two channels on its top surface following the same procedure described in 2.2.2.

3.2.3 Microbubble Preparation

For each day of experiments a new vial of microbubbles was prepared by suspending the contents in saline according to the manufacturer's instructions.

Four concentrations for SonoVue were tested: $2.5x10^2$, 10^3, $4x10^3$, and 10^4 microbubbles/mL. All new concentrations were prepared via serial dilution, in which 0.1 mL was withdrawn from the reconstituted vial and added to either 10 mL or 40 mL of deionized water. From this intermediate dilution, either 1 mL or 4 mL was withdrawn and added to 1 L of deionized water to produce the final working solution.

A single concentration of Sonazoid (GE Healthcare, Amersham, UK) was tested, 10^4 microbubbles/mL. The microbubbles were suspended according to the manufacturer's instructions and then the same serial dilution described above was used to prepare the final concentration.

The procedure to fill the box was the same as described in 2.2.4.

3.2.4 Data Collection Procedure

For each trial, a sweep of 10 acoustic pressures ranging from 70 kPa to 700 kPa was performed. Microbubbles were prepared and introduced into the box before the box was placed in the water tank. The box was then pressurized to the desired ambient pressure using a syringe. A single contrast-enhanced ultrasound loop of 5 frames was acquired to confirm microbubble quality, after which the system was switched to the subharmonic research mode and all acoustic pressures were tested sequentially.

To prevent signal saturation, after the fifth acoustic pressure, the imaging gain was reduced by 8 dB before continuing with the five higher acoustic pressures. Once all acoustic pressures were tested at a given ambient pressure, the box was emptied, refilled with a freshly prepared microbubble solution, and the procedure was repeated for the next ambient pressure.

Five ambient pressures were tested in total, ranging from 0 to 80 mmHg. This procedure was repeated for all microbubble concentrations and agents.

3.2.5 Data Analysis

Native DICOM files were collected and processed using QLAB software (Philips Healthcare, Bothell, WA, USA). A region of interest (ROI) was drawn spanning the width of the box at a depth of 5 to 7 cm (Figure 8). The average pixel intensity over 5 frames was calculated for each acquisition. When multiple trials were performed, the average intensity from each trial was averaged to produce a final value, and the standard deviation was calculated across trials.

To account for changes in gain between procedures, a conversion was applied in post-processing following the information from Lampaskis et. al [66]. This consisted of monitoring how much the gain changed by and then adding back the dB value of the gain change after processing.

3.3 Results

3.3.1 Subharmonic Response of SonoVue Over Varying Acoustic Pressure

When acoustic pressure was increased from 70 to 700 kPa, a positive relationship between acoustic pressure and subharmonic intensity was observed for SonoVue, although the shape differed from the classic three-stage S-curve observed in the single-element experiments. A sharp increase in subharmonic intensity was observed when increasing acoustic pressure from 70 to 170 kPa. The response then largely plateaued from 170 to 430 kPa before increasing sharply again between 430 and 700 kPa. These results are consistent with prior observations of SonoVue's acoustic pressure response [33], [36], [41], [44], [45], [46].

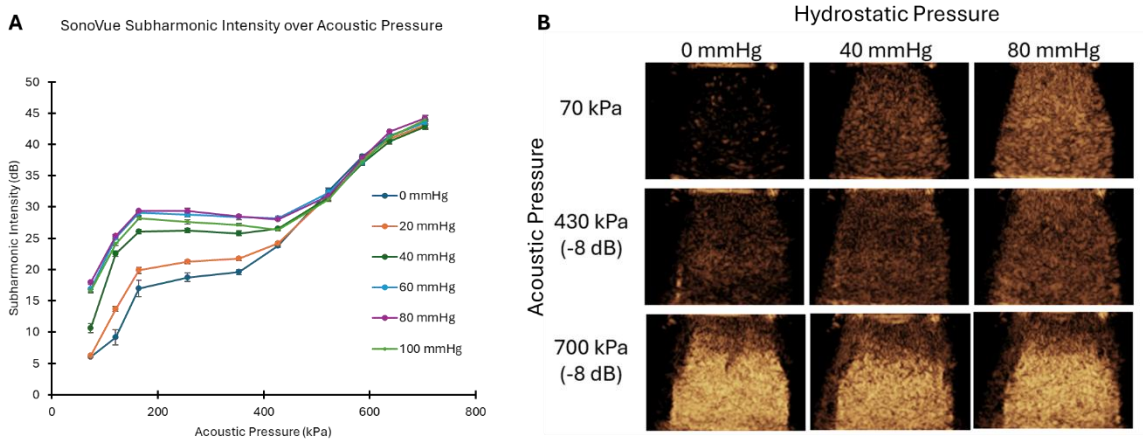

Figure 9: Subharmonic response of SonoVue in clinical system setup at a concentration of 10^4 microbubbles/mL. A) Subharmonic response of SonoVue as acoustic pressure increases at varying ambient pressure. B) SonoVue microbubbles imaged in subharmonic mode across different ambient and acoustic pressures. For higher acoustic pressures there is an 8 dB gain decrease to avoid saturation.

3.3.2 Subharmonic Response of SonoVue Over Varying Ambient Pressure

The relationship between ambient pressure and subharmonic intensity varied substantially depending on the acoustic pressure used. A positive relationship between ambient pressure and subharmonic intensity was observed across most conditions, but this relationship was considerably stronger at lower acoustic pressures. At the lowest acoustic pressure tested (70 kPa), a sensitivity of 0.54 dB/mmHg was observed between 20 and 40 mmHg. At a comparable ambient pressure range but 430 kPa acoustic pressure, sensitivity dropped to only 0.1 dB/mmHg. At acoustic pressures above 430 kPa, ambient pressure had little to no impact on subharmonic intensity.

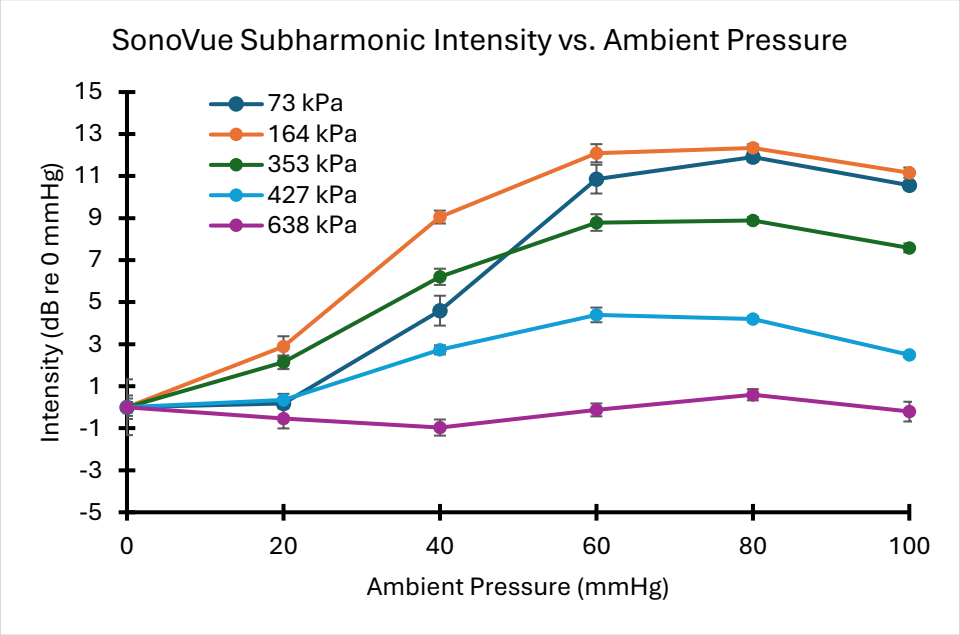

Figure 10: Subharmonic response of SonoVue at a concentration of 10^4 mB/mL vs ambient pressure at multiple acoustic pressures. All values are normalized to the intensity for the respective acoustic pressure at 0 mmHg.

3.3.3 Effect of Concentration on Subharmonic Response

The relationship between subharmonic response and acoustic pressure remained consistent regardless of concentration across the range tested. The change in subharmonic intensity with a tenfold change in concentration was comparable to that observed for the fundamental frequency, suggesting that the subharmonic responds to concentration similarly to other frequency components [66]. Sensitivity to ambient pressure also did not show a clear systematic pattern with concentration, indicating that concentration is not a meaningful confounding variable within the range tested.

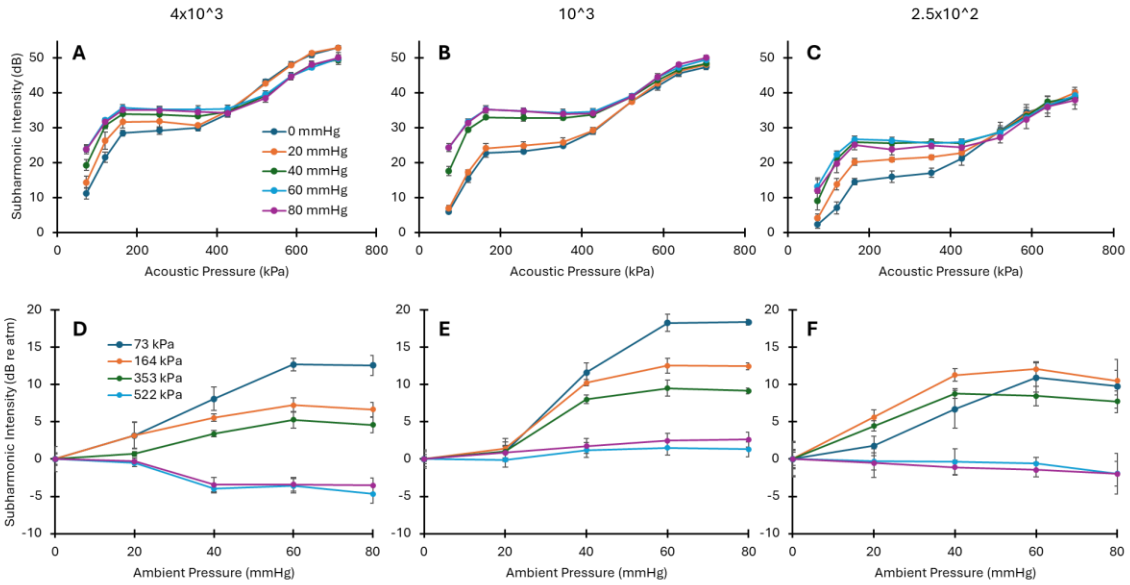

Figure 11: Response of SonoVue across concentrations

3.3.4 Comparison of SonoVue and Sonazoid

Sonazoid exhibited a substantially different response to both acoustic and ambient pressure compared to SonoVue. When acoustic pressure was increased, Sonazoid showed a generally positive and more linear relationship with subharmonic intensity than SonoVue, suggesting that a different mechanism may underlie subharmonic generation in Sonazoid compared to SonoVue.

Most significantly, Sonazoid showed little to no sensitivity to changes in ambient pressure. The largest change observed was at an acoustic pressure of 353 kPa, where a change of -4.5 dB was seen between 0 and 60 mmHg. However, this change was not consistent across the pressure range and no clear pattern was observed. This contrasts sharply with SonoVue, which showed a sensitivity of up to 0.54 dB/mmHg at low acoustic pressures.

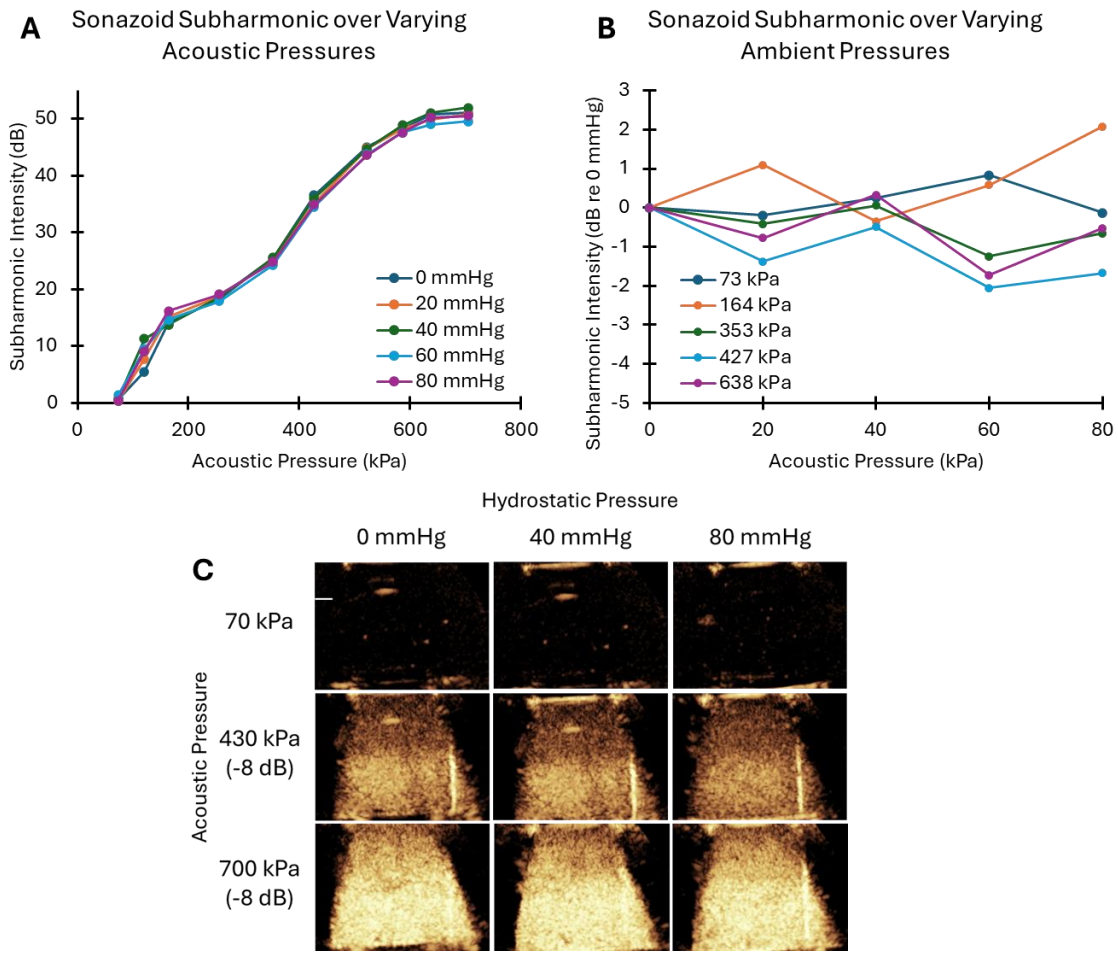

Figure 12: Sonazoid subharmonic response. A) Sonazoid subharmonic response as a function of acoustic pressure. B) Sonazoid subharmonic response as a function of ambient pressure. C) Images taken in subharmonic mode of Sonazoid microbubbles. For higher acoustic pressures there is an 8 dB gain decrease to avoid saturation.

3.4 Discussion

3.4.1 Interpretation of Clinical Machine Findings

The clinical machine experiments demonstrated that the positive subharmonic-ambient pressure relationship observed for SonoVue in Chapter 2 translates to a clinical imaging system, with important nuances regarding the dependence on acoustic pressure. The finding that

sensitivity is maximized at low acoustic pressures (70 kPa) is particularly significant for clinical translation. Previous clinical SHAPE work has often required patient-specific acoustic pressure optimization, and the strong sensitivity at low pressures suggests that a standardized low acoustic pressure protocol may be feasible for SonoVue-based SHAPE on a clinical system.

The shape of the acoustic pressure response on the clinical system differed from the classic S-curve observed with the single-element setup. Rather than the three clearly defined stages of occurrence, growth, and saturation, the clinical system showed a more complex response with two distinct regions of increasing sensitivity separated by a plateau. This may reflect differences in the pulse parameters, transducer characteristics, or signal processing between the two setups.

3.4.2 Comparison of SonoVue and Sonazoid

The most significant finding from this chapter is the stark difference in ambient pressure sensitivity between SonoVue and Sonazoid under identical experimental conditions. SonoVue showed strong, consistent sensitivity to ambient pressure at low acoustic pressures, while Sonazoid showed little to no sensitivity across the full range tested. This is a meaningful finding because the majority of current clinical SHAPE work has been conducted with Sonazoid, and the results presented here suggest that SonoVue may be a substantially more sensitive agent for pressure estimation under the conditions tested.

This difference likely reflects the distinct physical properties of each agent. SonoVue's phospholipid shell and perfluoropropane gas core give rise to compression-only behavior at low acoustic pressures [26], [38], which amplifies the sensitivity of the subharmonic response to

changes in ambient pressure. Sonazoid, which has a shell of hydrogenated egg phosphatidylserine sodium and perfluorobutane gas [67], does not exhibit the same degree of compression-only behavior, which may explain its relative insensitivity to ambient pressure under these conditions.

It is important to note that this comparison was conducted at a specific set of acoustic parameters and on a single clinical imaging system. It is possible that with different parameter optimization Sonazoid could show greater ambient pressure sensitivity, as prior literature has shown variable results across different experimental setups [44].

3.4.3 Concentration Effects

The consistency of the subharmonic-pressure relationship across concentrations is a practically important finding. It suggests that small variations in microbubble preparation or concentration between experiments are unlikely to substantially confound the pressure-dependent subharmonic signal within the range tested. This supports the feasibility of a standardized preparation protocol for clinical use, where precise concentration control may be difficult to achieve.

3.4.4 Comparison with Single-Element Findings

The clinical machine results are broadly consistent with the single-element findings in that SonoVue shows a positive relationship between subharmonic intensity and ambient pressure, maximized at low acoustic pressures. However, the ambient pressure range tested differed between the two setups. The sensitivity values also differed, which may reflect differences in

transducer characteristics, pulse parameters, and signal processing rather than a fundamental difference in microbubble behavior.

3.4.5 Limitations

As with the single-element experiments, these studies are limited by their in vitro nature. The absence of physiological flow means that microbubble populations within the imaging plane are not continuously replenished, and the static pressure conditions do not replicate the dynamic pressure changes experienced in vivo. Additionally, only a single clinical imaging system and transducer configuration were tested. Results may differ on other clinical platforms with different transducer properties or subharmonic imaging implementations.

The comparison between SonoVue and Sonazoid is also limited by the fact that the acoustic parameters were not independently optimized for each agent. It is possible that Sonazoid would show greater ambient pressure sensitivity under a different set of acoustic conditions. Finally, as with all work in this thesis, absolute pressure measurement was not achieved. The system can currently only measure relative pressure changes, which limits its immediate clinical utility.

Chapter 4. Discussion and Concluding Remarks

4.1 Summary of Main Findings

This thesis set out to establish a reproducible, experimental framework for characterizing the relationship between subharmonic magnitude and ambient pressure across multiple microbubble formulations, acoustic conditions, and concentrations, using both a single-element bench setup and a clinical imaging system. The central hypothesis was that with tightly controlled experimental conditions including suspension time, microbubble concentration, and acoustic pressure, a consistent and predictable subharmonic pressure relationship could be established.

The results from both phases of this work support this hypothesis. In the single-element transducer experiments described in Chapter 2, a reproducible and predictable relationship between subharmonic magnitude and ambient pressure was demonstrated for SonoVue under controlled bench-top conditions. The relationship was positive at low-to-moderate acoustic pressures and maximized at 150 kPa, with a peak sensitivity of 8.65 dB over the 0-150 mmHg range tested. In the clinical machine experiments described in Chapter 3, this relationship was successfully translated to a Philips EPIQ clinical imaging system, where SonoVue again showed strong positive ambient pressure sensitivity at low acoustic pressures, with a maximum sensitivity of 0.54 dB/mmHg observed at 70 kPa. Importantly, the subharmonic-pressure relationship remained consistent across a range of SonoVue concentrations, suggesting that concentration is not a meaningful confounding variable within the range tested. By contrast, Sonazoid showed little to no sensitivity to ambient pressure changes under the same

experimental conditions, a finding with significant implications for ongoing clinical SHAPE work.

4.2 Subharmonic-Pressure Relationship

4.2.1 Comparison of SonoVue Results Across Setups

Both experimental phases demonstrated a positive relationship between subharmonic intensity and ambient pressure for SonoVue, consistent with the theoretical prediction that increasing ambient pressure at low acoustic pressures emphasizes compression-only behavior and therefore enhances subharmonic generation [26], [38]. However, there were notable differences between the two setups in the shape and magnitude of the response.

In the single-element experiments, the acoustic pressure response followed the classic three-stage S-curve, occurrence, growth, and saturation, as described in prior literature [68]. The ambient pressure response showed a consistent trend across all three acoustic pressures tested, with subharmonic magnitude increasing from 0-50 mmHg, plateauing from 50-100 mmHg, and decreasing from 100-150 mmHg. On the clinical imaging system, the acoustic pressure response showed a more complex two-region shape rather than the classic S-curve, with two distinct regions of increasing sensitivity separated by a plateau. This aligns with results in other literature that has focused specifically on SonoVue [41], [57]. The differences in results likely reflect the differences in pulse parameters, transducer properties and signal processing rather than a fundamental difference in microbubble behavior.

The ambient pressure response was more consistent between the two setups. For both, SonoVue exhibited a positive relationship with ambient pressure from 0-80 mmHg and then the

relationship plateaued or decreased at higher ambient pressures. The translation of this between the two setups is particularly of note because this is the relationship that is necessary for ambient pressure sensing.

4.2.2 Microbubble Formulation Dependence

The subharmonic-pressure relationship was found to be highly dependent on microbubble formulation. SonoVue demonstrated strong and consistent positive ambient pressure sensitivity at low acoustic pressures across both setups, while Sonazoid showed little to no sensitivity to ambient pressure changes under identical conditions on the clinical imaging system. This stark difference likely reflects the distinct physical properties of each agent. SonoVue's unique phospholipid shell and perfluoropropane gas core give rise to compression-only behavior at low acoustic pressures [26], [38], which amplifies sensitivity to ambient pressure changes. Sonazoid, with its different shell and gas composition, does not exhibit the same degree of compression-only behavior, which may explain its relative insensitivity under the conditions tested.

It is possible that if the acoustic conditions were idealized for Sonazoid microbubbles a stronger relationship may be observed, but further testing would need to be completed. The results do show that SonoVue may be a powerful agent for ambient pressure sensing, as the sensitivity observed was still greater than what has been observed for Sonazoid at other acoustic conditions [40], [42], [69].

4.2.3 Comparison with Prior Literature

For SonoVue, the finding of a positive subharmonic-ambient pressure relationship at low acoustic pressures is consistent with prior work showing biphasic behavior — positive at low

acoustic pressures and negative at higher pressures [36], [44], [45]. The sensitivity values observed here (up to 0.54 dB/mmHg on the clinical system) are within the range reported in prior literature, though direct comparison is complicated by differences in acoustic parameters, imaging systems, and pressure ranges across studies. The more complex acoustic pressure response observed on the clinical system compared to the classic S-curve has also been noted in other clinical system implementations, likely reflecting the influence of transducer bandwidth and pulse compression on the received subharmonic signal [41].

For Sonazoid, the finding of minimal ambient pressure sensitivity is somewhat at odds with prior work which has shown a negative relationship between subharmonic amplitude and hydrostatic pressure, with sensitivities ranging from 0.02 to 0.22 dB/mmHg [42], [69]. The discrepancy may reflect differences in acoustic parameters, particularly the driving frequency used here relative to the Sonazoid resonance frequency, or differences in the imaging system used. This is an important distinction since much of the current clinical SHAPE work has used Sonazoid, and the low sensitivity observed here under these conditions suggests that careful parameter optimization is essential before Sonazoid can be used reliably for pressure estimation.

4.2.4 Implications for Parameter Standardization Across Scanners

A key challenge in the SHAPE field has been the lack of reproducibility across different labs and imaging systems, with studies reporting widely varying sensitivity values and even different directions of the subharmonic-pressure relationship depending on the conditions used [33], [44]. The results of this thesis address this challenge in two ways. First, by demonstrating tightly controlled experimental conditions including suspension time produce consistent and reproducible results both on a bench-top single-element setup and on a clinical imaging system.

Second, by identifying that low acoustic pressure is preferable for maximizing SonoVue sensitivity on a clinical system, which provides a concrete starting point for parameter standardization.

However, the differences in response shape and sensitivity between the two setups also highlight that parameters cannot be directly transferred between systems without validation. A standardized protocol for SHAPE on clinical imaging systems will need to account for system-specific differences in transducer characteristics, pulse parameters, and signal processing, and will require validation on multiple platforms before widespread adoption.

4.3 Effect of Concentration on Subharmonic Response

A key question motivating the concentration experiments in this thesis was whether variations in microbubble concentration between experiments could confound the observed subharmonic-pressure relationship, contributing to the inconsistency seen across studies in the field. The results suggest that within the range of concentrations tested (2.5×10^2 to 10^4 microbubbles/mL for SonoVue), concentration is not a meaningful confounding variable. The subharmonic-acoustic pressure relationship remained consistent across all concentrations, and the sensitivity to ambient pressure showed no clear pattern with concentration.

Furthermore, the change in subharmonic intensity with a tenfold change in concentration was comparable to that observed for the fundamental frequency [66], suggesting that the subharmonic responds to concentration in a similar way to other frequency components rather

than exhibiting a unique nonlinear concentration dependence that could complicate pressure estimation.

This finding is important for clinical translation. In a clinical setting, precise control of microbubble concentration is difficult or impossible to achieve due to an unknown volume of blood, changing local concentrations, and continuous microbubble degradation all influencing the concentration of microbubbles at the imaging plane. The knowledge that the subharmonic-pressure relationship is robust across a range of concentrations suggests that these clinical variables are unlikely to substantially confound pressure estimation, at least within the physiologically relevant concentration range explored here. This supports the feasibility of a standardized preparation and dosing protocol for clinical SHAPE without requiring precise concentration matching across patients or sessions.

4.4 Clinical Translation and Limitations

4.4.1 Successfully Conducting This Work on a Clinical Imaging System

One of the most significant contributions of this thesis is the successful translation of the subharmonic-pressure measurement framework to a Philips EPIQ clinical imaging system. Prior bench-top work, including the single-element experiments described in Chapter 2, provides important mechanistic insight but does not directly demonstrate that the technique is feasible on the type of hardware that would be used in a clinical setting. The clinical machine experiments described in Chapter 3 show that a meaningful and reproducible subharmonic-pressure relationship can be established on a real clinical system using clinically relevant hardware, pulse parameters, and data acquisition procedures. This represents a meaningful step toward clinical

implementation and suggests that the technique could be implemented as a software modification to an existing FDA-cleared imaging platform without requiring new hardware.

4.4.2 Limitations

Several important limitations of this work should be noted. All experiments were conducted in vitro using a pressurized acrylic chamber placed in a water tank. While this setup allowed for precise control of acoustic and ambient pressure conditions and enabled direct assessment of freshly prepared microbubbles, it eliminates many of the complexities present in vivo. In the body, large microbubbles are filtered by the lungs, microbubble dissipation rates are altered by physiological flow, and microbubbles are continuously replenished within the imaging plane as blood circulates. The static pressure conditions applied in this work also do not replicate the dynamic and pulsatile pressure changes that would be encountered in a clinical pressure measurement. It is possible that microbubbles respond differently under dynamic pressure conditions than under the static conditions applied here.

Only a single clinical imaging system and transducer configuration were evaluated. Results may differ on other clinical platforms with different transducer properties, pulse sequences, or subharmonic imaging implementations. The findings regarding optimal acoustic pressure and sensitivity values should therefore be treated as platform-specific until validated on additional systems. This lack of exploration across platforms also limits the applicability of this research to a widespread clinical method.

The most significant limitation of this work is the inability to measure absolute pressure. The subharmonic-pressure relationship established here is relative, meaning it can detect changes

in ambient pressure and distinguish between different pressure states, but cannot convert these to absolute pressure values without an external calibration reference. In the clinical context this means that a catheter-based calibration measurement would still be required to translate relative subharmonic changes into clinically meaningful absolute pressure values. Until this limitation is resolved, the technique cannot fully replace catheterization as a standalone diagnostic tool.

Finally, microbubble aging and suspension time were identified as important sources of variability. The finding in Chapter 2 that the observed relationship between subharmonic magnitude and ambient pressure changed substantially when suspension time was extended from three to eight minutes highlights the sensitivity of the technique to microbubble state. In a clinical setting where precise control of suspension time is difficult, this could be a meaningful source of variability that would need to be addressed through careful protocol design.

4.5 Future Work

Several directions for future work follow naturally from the findings of this thesis. The experiments described here were conducted under static ambient pressure conditions, where the applied pressure was held constant during each measurement. In the body, pressures are dynamic and pulsatile, cardiac pressures in particular change continuously with each heartbeat. The next important step is to evaluate the performance of the subharmonic-pressure relationship under dynamic pressure conditions. This could be achieved using a flow phantom in which both flow and cyclically changing ambient pressure can be applied simultaneously, providing conditions more closely resembling the in vivo environment. Evaluating whether the system can track real-

time pressure changes rather than just static pressure states would be an essential step toward clinical translation.

In vivo animal model validation is another critical future direction. While the in vitro results presented here provide strong proof of concept, translation to in vivo conditions will introduce the physiological complexities that were excluded from this work, including microbubble filtering by the lungs, physiological flow, tissue attenuation, and dynamic pressure variations. Animal model experiments, likely beginning with a large animal model where cardiac catheterization can be performed simultaneously for comparison, would provide the next level of validation needed before human studies can be considered.

The most significant barrier to clinical utility identified in this work is the inability to measure absolute pressure. A promising approach to resolving this limitation has been proposed by Spiekhout et al. [70], which involves the use of a low-frequency transducer, synchronized with the imaging system to provide known amplitude modulation. When microbubbles experience this low-frequency modulation, the resulting change in subharmonic intensity can be used to determine the slope of the subharmonic-pressure curve at the operating point, which in turn corresponds to a unique absolute pressure value. Implementing and validating this approach on the clinical imaging system described in this thesis would be a high-priority next step, as it has the potential to eliminate the need for catheter-based calibration entirely.

4.6 Concluding Remarks

This thesis set out to establish whether a consistent and predictable relationship between subharmonic magnitude and ambient pressure could be demonstrated using both a single-element bench-top setup and a clinical imaging system. The results support this goal. A reproducible subharmonic-pressure relationship was demonstrated for SonoVue across both experimental phases, with tightly controlled conditions found to be essential for consistency. The relationship was successfully translated to a Philips EPIQ clinical imaging system, where SonoVue showed meaningful ambient pressure sensitivity at low acoustic pressures. Microbubble concentration was found not to be a meaningful confounding variable within the range tested, supporting the feasibility of a standardized clinical protocol. The comparison between SonoVue and Sonazoid revealed a stark difference in ambient pressure sensitivity, with SonoVue substantially outperforming Sonazoid under the conditions tested, a finding with direct implications for ongoing clinical SHAPE work that has predominantly used Sonazoid.

Taken together, these findings represent a meaningful step toward a fully non-invasive hydrostatic pressure measurement technique. The successful demonstration of the subharmonic-pressure relationship on a clinical imaging system with high reliability and sensitivity, along with the knowledge that concentration is not an important confounding factor, important progress towards a non-invasive pressure measurement.

References

[1] "Right Heart Catheterization: Procedure Details and Results," Cleveland Clinic. Accessed: May 06, 2024. [Online]. Available: https://my.clevelandclinic.org/health/diagnostics/21045-right-heart-catheterization

[2] K. Chatterjee, "The Swan-Ganz Catheters: Past, Present, and Future," *Circulation*, vol. 119, no. 1, pp. 147–152, Jan. 2009, doi: 10.1161/CIRCULATIONAHA.108.811141.

[3] S. M. Haleem, T. Sharma, and S. S. Chaudhari, "Right Heart Catheterization," *StatPearls*, Jul. 2025, Accessed: May 24, 2026. [Online]. Available: https://www.ncbi.nlm.nih.gov/books/NBK557404/

[4] D. E. Kaplan *et al.*, "AASLD Practice Guidance on risk stratification and management of portal hypertension and varices in cirrhosis," *Hepatology*, vol. 79, no. 5, pp. 1180–1211, May 2024, doi: 10.1097/HEP.0000000000000647.

[5] C. H. Heldin, K. Rubin, K. Pietras, and A. Östman, "High interstitial fluid pressure — an obstacle in cancer therapy," *Nature Reviews Cancer 2004 4:10*, vol. 4, no. 10, pp. 806–813, Oct. 2004, doi: 10.1038/nrc1456.

[6] G. W. J. Hawryluk *et al.*, "Intracranial pressure: current perspectives on physiology and monitoring," *Intensive Care Medicine 2022 48:10*, vol. 48, no. 10, pp. 1471–1481, Jul. 2022, doi: 10.1007/S00134-022-06786-Y.

[7] B. Alexander, M. Cannesson, and T. J. Quill, *Blood Pressure Monitoring*. W.B. Saunders, 2013. doi: 10.1016/B978-0-323-11237-6.00012-1.

[8] A. F. Connors *et al.*, "The Effectiveness of Right Heart Catheterization in the Initial Care of Critically III Patients," *JAMA*, vol. 276, no. 11, pp. 889–897, Sep. 1996, doi: 10.1001/JAMA.1996.03540110043030.

[9] Y. R. Manda and K. M. Baradhi, "Cardiac Catheterization Risks and Complications," *StatPearls*, Jun. 2023, Accessed: May 08, 2026. [Online]. Available: https://www.ncbi.nlm.nih.gov/books/NBK531461/

[10] H. J. C. Swan, W. Ganz, J. Forrester, H. Marcus, G. Diamond, and D. Chonette, "Catheterization of the Heart in Man with Use of a Flow-Directed Balloon-Tipped Catheter," *New England Journal of Medicine*, vol. 283, no. 9, pp. 447–451, Aug. 1970, doi: 10.1056/NEJM197008272830902;SUBPAGE:STRING:ACCESS.

[11] R. A. Archbold, N. M. Robinson, and R. J. Schilling, "Radial artery access for coronary angiography and percutaneous coronary intervention," *BMJ : British Medical Journal*, vol. 329, no. 7463, p. 443, Aug. 2004, doi: 10.1136/BMJ.329.7463.443.

[12] G. Savarese, P. M. Becher, L. H. Lund, P. Seferovic, G. M. C. Rosano, and A. J. S. Coats, "Global burden of heart failure: a comprehensive and updated review of epidemiology," *Cardiovasc. Res.*, vol. 118, no. 17, pp. 3272–3287, Jan. 2023, doi: 10.1093/CVR/CVAC013.

[13] M. Arrigo *et al.*, “Acute heart failure,” *Nature Reviews Disease Primers 2020 6:1*, vol. 6, no. 1, pp. 16-, Mar. 2020, doi: 10.1038/s41572-020-0151-7.

[14] P. J. Leary *et al.*, “Global, regional, and national burden of pulmonary arterial hypertension, 1990–2021: a systematic analysis for the Global Burden of Disease Study 2021,” *Lancet Respir. Med.*, vol. 13, no. 1, pp. 69–79, Jan. 2025, doi: 10.1016/S2213-2600(24)00295-9.

[15] S. Rosenkranz, L. S. Howard, M. Gomberg-Maitland, and M. M. Hoeper, “Systemic Consequences of Pulmonary Hypertension and Right-Sided Heart Failure,” *Circulation*, vol. 141, no. 8, pp. 678–693, Feb. 2020, doi: 10.1161/CIRCULATIONAHA.116.022362.

[16] P. Ginès, A. Krag, J. G. Abraldes, E. Solà, N. Fabrellas, and P. S. Kamath, “Liver cirrhosis,” *The Lancet*, vol. 398, no. 10308, pp. 1359–1376, Oct. 2021, doi: 10.1016/S0140-6736(21)01374-X.

[17] Q. Lu *et al.*, “Hepatic venous-portal gradient (HVPG) measurement: pearls and pitfalls,” *Br. J. Radiol.*, vol. 94, no. 1124, p. 20210061, Aug. 2021, doi: 10.1259/BJR.20210061.

[18] B. V. Scheer, A. Perel, and U. J. Pfeiffer, “Clinical review: Complications and risk factors of peripheral arterial catheters used for haemodynamic monitoring in anaesthesia and intensive care medicine,” *Crit. Care*, vol. 6, no. 3, p. 199, 2002, doi: 10.1186/CC1489.

[19] M. J. Albeck, S. E. Borgesen, F. Gjerris, J. F. Schmidt, and P. S. Sorensen, “Intracranial pressure and cerebrospinal fluid outflow conductance in healthy subjects,” *J. Neurosurg.*, vol. 74, no. 4, pp. 597–600, 1991, doi: 10.3171/JNS.1991.74.4.0597.

[20] M. A. Averkiou, M. F. Bruce, J. E. Powers, P. S. Sheeran, and P. N. Burns, "Imaging Methods for Ultrasound Contrast Agents," *Ultrasound Med. Biol.*, vol. 46, no. 3, pp. 498–517, Mar. 2020, doi: 10.1016/j.ultrasmedbio.2019.11.004.

[21] M. A. Averkiou, D. N. Roundhill, and J. E. Powers, "New imaging technique based on the nonlinear properties of tissues," *Proceedings of the IEEE Ultrasonics Symposium*, vol. 2, pp. 1561–1566, 1997, doi: 10.1109/ULTSYM.1997.663294.

[22] A. L. Klibanov, "Ultrasound Contrast: Gas Microbubbles in the Vasculature," *Invest. Radiol.*, vol. 56, no. 1, pp. 50–61, Jan. 2021, doi: 10.1097/RLI.0000000000000733.

[23] V. Paefgen, D. Doleschel, and F. Kiessling, "Evolution of contrast agents for ultrasound imaging and ultrasound-mediated drug delivery," *Front. Pharmacol.*, vol. 6, no. SEP, p. 150978, Sep. 2015, doi: 10.3389/FPHAR.2015.00197/FULL.

[24] E. A. Neppiras, "Acoustic cavitation," *Phys. Rep.*, vol. 61, no. 3, pp. 159–251, May 1980, doi: 10.1016/0370-1573(80)90115-5.

[25] J. Henderson, K. Willson, J. R. Jago, and T. A. Whittingham, "A survey of the acoustic outputs of diagnostic ultrasound equipment in current clinical use," *Ultrasound Med. Biol.*, vol. 21, no. 5, pp. 699–705, Jan. 1995, doi: 10.1016/0301-5629(94)00158-A.

[26] P. Marmottant *et al.*, "A model for large amplitude oscillations of coated bubbles accounting for buckling and rupture," *J. Acoust. Soc. Am.*, vol. 118, no. 6, pp. 3499–3505, Dec. 2005, doi: 10.1121/1.2109427.

[27] Q. Wu *et al.*, "Challenges in classifying cavitation: Correlating high-speed optical imaging and passive acoustic mapping of cavitation dynamics," *J. Acoust. Soc. Am.*, vol. 156, no. 5, pp. 3608–3620, Nov. 2024, doi: 10.1121/10.0034426.

[28] C. C. Coussios and R. A. Roy, "Applications of acoustics and cavitation to noninvasive therapy and drug delivery," *Annu. Rev. Fluid Mech.*, vol. 40, no. Volume 40, 2008, pp. 395–420, Jan. 2008, doi: 10.1146/ANNUREV.FLUID.40.111406.102116/CITE/REFWORKS.

[29] P. M. Shankar, P. D. Krishna, and V. L. Newhouse, "Advantages of Subharmonic Over Second Harmonic Backscatter for Contrast-To-Tissue Echo Enhancement," *Ultrasound Med. Biol.*, vol. 24, no. 3, pp. 395–399, Mar. 1998, doi: 10.1016/S0301-5629(97)00262-7.

[30] W. T. Shi, F. Forsberg, J. S. Raichlen, L. Needleman, and B. B. Goldberg, "Pressure dependence of subharmonic signals from contrast microbubbles," *Ultrasound Med. Biol.*, vol. 25, no. 2, pp. 275–283, Feb. 1999, doi: 10.1016/S0301-5629(98)00163-X.

[31] E. Kimmel, B. Krasovitski, A. Hoogi, D. Razansky, and D. Adam, "Subharmonic Response of Encapsulated Microbubbles: Conditions for Existence and Amplification," *Ultrasound Med. Biol.*, vol. 33, no. 11, pp. 1767–1776, Nov. 2007, doi: 10.1016/J.ULTRASMEDBIO.2007.05.011.

[32] W. T. Shi, F. Forsberg, J. S. Raichlen, L. Needleman, and B. B. Goldberg, "Pressure dependence of subharmonic signals from contrast microbubbles," *Ultrasound Med. Biol.*, vol. 25, no. 2, pp. 275–283, Feb. 1999, doi: 10.1016/S0301-5629(98)00163-X.

[33] I. Gupta, J. R. Eisenbrey, P. Machado, M. Stanczak, K. Wallace, and F. Forsberg, "On Factors Impacting Subharmonic Aided Pressure Estimation (SHAPE)," *Ultrason. Imaging*, vol. 41, no. 1, p. 35, Jan. 2018, doi: 10.1177/0161734618812083.

[34] A. Katiyar and K. Sarkar, "Excitation threshold for subharmonic generation from contrast microbubbles," *J. Acoust. Soc. Am.*, vol. 130, no. 5, p. 3137, Nov. 2011, doi: 10.1121/1.3641455.

[35] J. Chomas, P. Dayton, D. May, and K. Ferrara, "Nondestructive subharmonic imaging," *IEEE Trans. Ultrason. Ferroelectr. Freq. Control*, vol. 49, no. 7, pp. 883–892, Jul. 2002, doi: 10.1109/TUFFC.2002.1020158.

[36] X. Qiao, Y. Wen, J. Yu, A. Bouakaz, Y. Zong, and M. Wan, "Noninvasive Pressure Estimation Based on the Subharmonic Response of SonoVue: Application to Intracranial Blood Pressure Assessment," *IEEE Trans. Ultrason. Ferroelectr. Freq. Control*, vol. 69, no. 3, pp. 957–966, Mar. 2022, doi: 10.1109/TUFFC.2021.3138100.

[37] C. Tremblay-Darveau, R. Williams, and P. N. Burns, "Measuring absolute blood pressure using microbubbles," *Ultrasound Med. Biol.*, vol. 40, no. 4, pp. 775–787, Apr. 2014, doi: 10.1016/j.ultrasmedbio.2013.10.017.

[38] N. de Jong *et al.*, "'Compression-Only' Behavior of Phospholipid-Coated Contrast Bubbles," *Ultrasound Med. Biol.*, vol. 33, no. 4, pp. 653–656, Apr. 2007, doi: 10.1016/j.ultrasmedbio.2006.09.016.

[39] P. J. A. Frinking, E. Gaud, J. Brochot, and M. Arditi, “Subharmonic scattering of phospholipid-shell microbubbles at low acoustic pressure amplitudes,” *IEEE Trans. Ultrason. Ferroelectr. Freq. Control*, vol. 57, no. 8, pp. 1762–1771, Aug. 2010, doi: 10.1109/TUFFC.2010.1614.

[40] K. Kalayeh *et al.*, “A Comparative Study of Commercially Available Ultrasound Contrast Agents for Sub-harmonic-Aided Pressure Estimation (SHAPE) in a Bladder Phantom,” *Ultrasound Med. Biol.*, vol. 50, no. 10, pp. 1494–1505, Oct. 2024, doi: 10.1016/j.ultrasmedbio.2024.05.019.

[41] H. Mayer *et al.*, “Investigation Into the Subharmonic Response of Three Contrast Agents in Static and Dynamic Flow Environments Using a Commercially Available Diagnostic Ultrasound Scanner,” *Ultrasound Med. Biol.*, vol. 50, no. 11, pp. 1731–1738, Nov. 2024, doi: 10.1016/j.ultrasmedbio.2024.07.015.

[42] V. G. Halldorsdottir *et al.*, “Subharmonic Contrast Microbubble Signals for Noninvasive Pressure Estimation Under Static and Dynamic Flow Conditions,” *Ultrason. Imaging*, vol. 33, no. 3, p. 153, 2011, doi: 10.1177/016173461103300301.

[43] I. Gupta, J. R. Eisenbrey, P. Machado, M. Stanczak, K. Wallace, and F. Forsberg, “On Factors Affecting Subharmonic-aided Pressure Estimation (SHAPE),” *Ultrason. Imaging*, vol. 41, no. 1, pp. 35–48, Jan. 2019, doi: 10.1177/0161734618812083.

[44] R. H. Azami, F. Forsberg, J. R. Eisenbrey, and K. Sarkar, “Ambient Pressure Sensitivity of the Subharmonic Response of Coated Microbubbles: Effects of Acoustic Excitation

Parameters," *Ultrasound Med. Biol.*, vol. 49, no. 7, pp. 1550–1560, Jul. 2023, doi: 10.1016/J.ULTRASMEDBIO.2023.02.019.

[45] G. Xu *et al.*, "Portal Vein Pressure Estimation and Portal Hypertension Discrimination Based on Subharmonic Scattering of Ultrasound Contrast Agent Microbubbles," *IEEE Trans. Biomed. Eng.*, vol. 71, no. 1, pp. 150–159, Jan. 2024, doi: 10.1109/TBME.2023.3293952.

[46] A. Q. X. Nio *et al.*, "Optimal Control of SonoVue Microbubbles to Estimate Hydrostatic Pressure," *IEEE Trans. Ultrason. Ferroelectr. Freq. Control*, vol. 67, no. 3, p. 557, Mar. 2019, doi: 10.1109/TUFFC.2019.2948759.

[47] Y. Chen *et al.*, "Explaining the correlation between subharmonic amplitude and ambient pressure for subharmonic-aided pressure estimation (SHAPE)," *Applied Acoustics*, vol. 227, p. 110235, Jan. 2025, doi: 10.1016/J.APACOUST.2024.110235.

[48] F. Forsberg, J.-B. Liu, W. T. Shi, J. Furuse, M. Shimizu, and B. B. Goldberg, "In Vivo Pressure Estimation Using Subharmonic Contrast Microbubble Signals: Proof of Concept," *IEEE Trans. Ultrason. Ferroelectr. Freq. Control*, vol. 52, no. 4, pp. 581–583, 2005, doi: 10.1109/tuffc.2005.1428040.

[49] J. K. Dave *et al.*, "Noninvasive LV Pressure Estimation Using Subharmonic Emissions From Microbubbles," *JACC Cardiovasc. Imaging*, vol. 5, no. 1, pp. 87–92, Jan. 2012, doi: 10.1016/J.JCMG.2011.08.017.

[50] J. K. Dave *et al.*, "Subharmonic microbubble emissions for noninvasively tracking right ventricular pressures," *Am. J. Physiol. Heart Circ. Physiol.*, vol. 303, no. 1, p. H126, Jul. 2012, doi: 10.1152/AJPHEART.00560.2011.

[51] J. K. Dave *et al.*, "Non-Invasive Intra-cardiac Pressure Measurements Using Subharmonic-Aided Pressure Estimation: Proof of Concept in Humans," *Ultrasound Med. Biol.*, vol. 43, no. 11, pp. 2718–2724, Nov. 2017, doi: 10.1016/j.ultrasmedbio.2017.07.009.

[52] C. Esposito, K. Dickie, F. Forsberg, and J. K. Dave, "Developing an Interface and Investigating Optimal Parameters for Real-Time Intra-Cardiac Subharmonic Aided Pressure Estimation," *IEEE Trans. Ultrason. Ferroelectr. Freq. Control*, vol. 68, no. 3, p. 579, Mar. 2021, doi: 10.1109/TUFFC.2020.3016264.

[53] C. Esposito *et al.*, "Noninvasive Evaluation of Cardiac Chamber Pressures Using Subharmonic-Aided Pressure Estimation With Definity Microbubbles," *JACC Cardiovasc. Imaging*, vol. 16, no. 2, pp. 224–235, Feb. 2023, doi: 10.1016/J.JCMG.2022.09.013.

[54] C. Esposito *et al.*, "Evaluation of Intracardiac Pressures Using Subharmonic-aided Pressure Estimation with Sonazoid Microbubbles," *https://doi.org/10.1148/ryct.230153*, vol. 6, no. 1, Feb. 2024, doi: 10.1148/RYCT.230153.

[55] J. K. Dave *et al.*, “Investigating the Efficacy of Subharmonic Aided Pressure Estimation for Portal Vein Pressures and Portal Hypertension Monitoring,” *Ultrasound Med. Biol.*, vol. 38, no. 10, pp. 1784–1798, Oct. 2012, doi: 10.1016/j.ultrasmedbio.2012.06.013.

[56] J. R. Eisenbrey *et al.*, “Chronic liver disease : Noninvasive subharmonic aided pressure estimation of hepatic venous pressure gradient,” *Radiology*, vol. 268, no. 2, pp. 581–588, Aug. 2013, doi: 10.1148/RADIOL.13121769/-/DC1.

[57] R. H. Azami, F. Forsberg, J. R. Eisenbrey, and K. Sarkar, “Acoustic response and ambient pressure sensitivity characterization of SonoVue for noninvasive pressure estimation,” *J. Acoust. Soc. Am.*, vol. 155, no. 4, p. 2636, Apr. 2024, doi: 10.1121/10.0025690.

[58] A. Needles *et al.*, “NONLINEAR CONTRAST IMAGING WITH AN ARRAY-BASED MICRO-ULTRASOUND SYSTEM,” *Ultrasound Med. Biol.*, vol. 36, no. 12, pp. 2097–2106, 2010, doi: 10.1016/j.ultrasmedbio.2010.08.012.

[59] V. Daeichin, J. G. Bosch, A. Needles, F. S. Foster, A. van der Steen, and N. de Jong, “Subharmonic, non-linear fundamental and ultraharmonic imaging of microbubble contrast at high frequencies,” *Ultrasound Med. Biol.*, vol. 41, no. 2, pp. 486–497, Feb. 2015, doi: 10.1016/j.ultrasmedbio.2014.10.003.

[60] M. Averkiou *et al.*, “Quantification of Tumor Microvascularity with Respiratory Gated Contrast Enhanced Ultrasound for Monitoring Therapy,” *Ultrasound Med. Biol.*, vol. 36, no. 1, pp. 68–77, Jan. 2010, doi: 10.1016/J.ULTRASMEDBIO.2009.07.005.

[61] "Marketing Clearance of Diagnostic Ultrasound Systems and Transducers," FDA. Accessed: May 28, 2024. [Online]. Available: https://www.fda.gov/regulatory-information/search-fda-guidance-documents/marketing-clearance-diagnostic-ultrasound-systems-and-transducers

[62] R. S. Meltzer, "Food and Drug Administration ultrasound device regulation: the output display standard, the 'mechanical index,' and ultrasound safety," *J. Am. Soc. Echocardiogr.*, vol. 9, no. 2, pp. 216–220, 1996, doi: 10.1016/S0894-7317(96)90035-8.

[63] E. Ashley and J. Niebauer, "Cardiology Explained," in *Understanding the echocardiogram*, London: Remedica, 2004, ch. 4.

[64] J.-M. Gorce, M. Arditi, and M. Schneider, "Influence of Bubble Size Distributions on the Echogenicity of Ultrasound Contrast Agents A Study of SonoVue," *Invest. Radiol.*, vol. 35, no. 11, pp. 661–671, Nov. 2000, doi: 10.1097/00004424-200011000-00003.

[65] S. B. Keller, P. S. Sheeran, and M. A. Averkiou, "Cavitation therapy monitoring of commercial microbubbles with a clinical scanner," *IEEE Trans. Ultrason. Ferroelectr. Freq. Control*, vol. 68, no. 4, pp. 1144–1154, Apr. 2021, doi: 10.1109/TUFFC.2020.3034532.

[66] M. Lampaskis and M. Averkiou, "Investigation of the Relationship of Nonlinear Backscattered Ultrasound Intensity with Microbubble Concentration at Low MI," *Ultrasound Med. Biol.*, vol. 36, no. 2, pp. 306–312, Feb. 2010, doi: 10.1016/J.ULTRASMEDBIO.2009.09.011.

[67] X. Li *et al.*, “Dynamic Contrast-Enhanced Ultrasonography with Sonazoid for Diagnosis of Microvascular Invasion in Hepatocellular Carcinoma,” *Ultrasound Med. Biol.*, vol. 48, no. 3, pp. 575–581, Mar. 2022, doi: 10.1016/J.ULTRASMEDBIO.2021.11.005.

[68] W. T. Shi and F. Forsberg, “Ultrasonic characterization of the nonlinear properties of contrast microbubbles,” *Ultrasound Med. Biol.*, vol. 26, no. 1, pp. 93–104, Jan. 2000, doi: 10.1016/S0301-5629(99)00117-9.

[69] T. Faez, G. Renaud, M. Defontaine, S. Calle, and N. De Jong, “Dynamic manipulation of the subharmonic scattering of phospholipid-coated microbubbles,” *Phys. Med. Biol.*, vol. 56, no. 19, p. 6459, Sep. 2011, doi: 10.1088/0031-9155/56/19/018.

[70] S. Spiekhout, J. Voorneveld, N. de Jong, and J. G. Bosch, “Dual-Frequency Subharmonic Ultrasound Contrast Imaging for Non-Invasive Blood Pressure Measurement,” *Ultrasound Med. Biol.*, vol. 51, no. 5, pp. 870–876, May 2025, doi: 10.1016/J.ULTRASMEDBIO.2025.01.015.